The Journal of Chemical Physics

Sulfurous and Sulfonic Acids: Predicting the Infrared Spectrum and Setting the Surface Straight

Jonathon P. Misiewicz, Kevin B. Moore III, Peter R. Franke, W. James Morgan, Justin M. Turney, Gary E. Douberly, and Henry F. Schaefer III[a)]

(Dated: 12 December 2019)

Sulfurous acid (H_2SO_3) is an infamously elusive molecule. Although some theoretical papers have supposed possible roles for it in more complicated systems, it has yet to be experimentally observed. To aid experiment in detecting this molecule, we have examined the H_2O+SO_2 potential energy surface at the CCSDT(Q)/CBS//CCSD(T)-F12b/cc-pVTZ-F12b level of theory to resolve standing discrepancies in previous reports and predict the gas-phase vibrational spectrum for H_2SO_3. We find that sulfurous acid has two potentially detectable rotamers, separated by 1.1 kcal mol^{-1} ΔH_{0K} with a torsional barrier of 1.6 kcal mol^{-1}. The sulfonic acid isomer is only 6.9 kcal mol^{-1} above the lowest enthalpy sulfurous acid rotamer, but the barrier to form it is 57.2 kcal mol^{-1}. Error in previous reports can be attributed to misidentified stationary points, the use of density functionals that perform poorly for this system, and most importantly the basis set sensitivity of sulfur. Using VPT2+K, we determine that the intense S=O stretch fundamental of each species is separated from other intense peaks by at least 25 cm^{-1}, providing a target for identification by infrared spectroscopy.

[a)]ccq@uga.edu

I. INTRODUCTION

Liedl and coworkers[1] contended in 2002 that the isolation and characterization of neutral sulfurous acid [$OS(OH)_2$] (Figures 1a and 1b) was one of the greatest open challenges in inorganic chemistry. The only characterization at that time was a mass spectrum of $OS(OH)_2$ obtained after

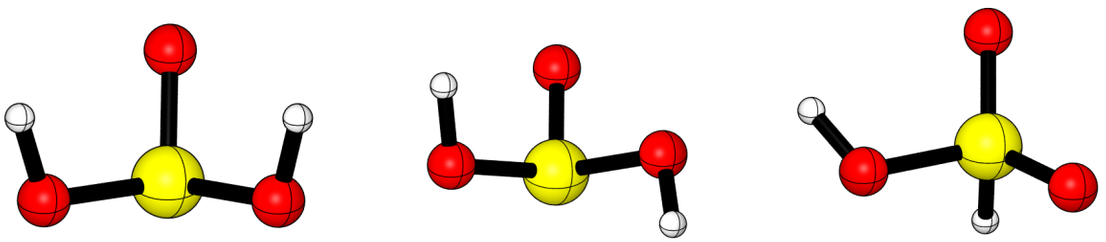

(a) *cis*-sulfurous acid (b) *trans*-sulfurous acid (c) sulfonic acid

FIG. 1: The geometries of *cis*-sulfurous acid (a), *trans*-sulfurous acid (b), and sulfonic acid (c).

neutralization and reionization of the cation.[2] Since that time, the infrared spectrum of the $S(OH)_3^+$ cation has been reported,[3] but $OS(OH)_2$ continues to elude experimental observation. Infrared and Raman spectroscopy have failed to find it in solution, instead reporting solvated SO_2 or HSO_3^-.[4–7] XANES has been used to probe solutions over a wide range of pH, but experimenters found aqueous SO_2 instead of sulfurous acid.[8] Spectrophotometric titration reported the same result.[9] Experimental acidities and thermochemical parameters all agree that product sulfurous acid in solution is both kinetically and thermodynamically unfavorable.[10–14]

Efforts to find sulfurous acid outside of solution have primarily found a van der Waals complex between SO_2 and H_2O. Matrix isolation experiments have detected a complex between the two, as determined by vibrational frequency shifts of the constituent monomers, but no product has been reported.[15–18] A $SO_2 \cdots H_2O$ complex has also been found at the air/water surface.[19,20] The complex has even been found in the gas phase, and its geometry was determined from least-squares fitting to moments of inertia obtained by microwave spectroscopy.[21] The photoionization spectrum[22] and excited states[23] of $SO_2 \cdots H_2O$ have also been studied. Yet sulfurous acid remains unobserved.

It was speculated that proton implantation could form detectable quantities of sulfurous acid on the Jovian moon Io,[24] but proton implantation experiments on SO_2 ices that simulate those on Io did not yield infrared spectra consistent with sulfurous acid.[25] This finding is in accordance

with estimates from the the rate of proton implantation.[26] The HSO_3^- anion can be found in such experiments, but not sulfurous acid itself.[27,28]

Experimental[29,30] and theoretical[30–37] studies have also tried to discern its atmospheric importance, often assuming that the molecule can still serve as a nucleation center for aerosols despite the lack of unambiguous experimental observation. Two such investigations are worthy of special note. First, a recent study by Choi, Kang, and coworkers[38] has found theoretical evidence for formation of sulfurous acid from SO_2 adsorbed on ice surfaces with a low energy barrier. Second, Donaldson, Kroll, and Vaida[30] hypothesized that triplet SO_2 can react with water to form sulfurous acid, based on a transition state leading to sulfurous acid in the triplet state. Later studies of $SO_2 + H_2O$ reactions[39,40] have found only hydroxyl radical elimination transition states. Our own research indicates that the transition state of reference 30 does not lead to sulfurous acid, but it is instead one of the hydroxyl radical formation transition states. We are not the first to recognize this.[41] This issue is discussed further in the SI. Nonetheless, the lack of experimental evidence of sulfurous acid and the recent theoretical confusion of reference 30 highlights the need for careful consideration of the $SO_2 + H_2O$ surface as a whole. This is especially true as it pertains to the formation of sulfurous acid and possible spectroscopic identification.

The vast majority of the information we have about the $SO_2 + H_2O$ system, sulfurous acid included, is from theoretical studies. Theory has been used to predict the geometry and thermochemistry of stationary points on the sulfurous acid potential energy surface,[18,21,30,33,42–56] the harmonic vibrational frequencies of sulfurous acid,[54,57] its molecular dynamics,[58–64] the rate constants of sulfurous acid consuming and producing reactions,[1,34,35,65–67] and the role of sulfurous acid in larger systems.[32,36,68–70]

The consensus of these studies is that in the gas-phase, the $SO_2 \cdots H_2O$ complex is lower in energy than sulfurous acid,[1,33–35,47,48,50,51,65,69] which makes sulfurous acid thermodynamically unfavorable. Further, the barrier to dissociation decreases in the presence of catalytic water,[1,33,35,47,50,65,69] making equilibration increasingly rapid. However, in the gas phase, sulfurous acid must surmount a barrier of approximately 30 kcal mol^{-1} to decompose.[1,33–35,47,50,65,69] Once gas-phase sulfurous acid is produced, it may persist long enough for spectroscopic identification, depending on experimental conditions. Spectroscopic identification of sulfurous acid would provide an important basic check on claims of the acid's importance in more complicated systems. However, synthesizing the previous studies leads to important questions for any attempt

at experimental identification.

1. Previous research reported two rotamers of sulfurous acid.[1,32,44,49,51] Are both sulfurous acid rotamers and the transition state connecting them energetically low-lying enough for both rotamers to have significant populations? The *cis* rotamer (Figure 1a) has both hydrogens pointing in the same direction, and the *trans* rotamer (Figure 1b) has the hydrogens pointing in opposite directions. Previous studies have found that the *cis* rotamer is energetically favored, but the *trans* rotamer is still low-lying. It has been reported to be 1.1 kcal mol^{-1} higher both in $\Delta G_{298\mathrm{K}}$ at QCISD(T)//MP2/6-311++G(3df,2p),[49] 0.9 kcal mol^{-1} higher in $\Delta H_{0\mathrm{K}}$ at B3LYP/6-311++G(3df,3pd),[32] and 1.0 kcal mol^{-1} higher in electronic energy at CCSD(T)//MP2/aug-cc-pVTZ.[1] However, there has only been one report of the torsional barrier, predicted to lie 2.4 kcal mol^{-1} above the *cis* rotamer at CCSD(T)//MP2/aug-cc-pVTZ without zero-point corrections. For compounds containing second row main-group elements, including sulfur, it is known that the correlation consistent basis sets converge very slowly unless additional tight d functions are included.[71] That is, achieving the quality expected of aug-cc-pVTZ requires the special aug-cc-pV(T+d)Z basis set when sulfur is present. At the triple-ζ level, excluding the tight d functions can cause errors over 2.2 kcal mol^{-1} for electronic energy differences of isomers.[72] If the torsional barrier is sensitive to choice of basis set, then a basis set including tight d functions will be necessary to assess whether this second rotamer is energetically accessible.

2. Does a third sulfurous acid rotamer exist? Li, Bu, and coworkers reported a third rotamer 3.2 kcal mol^{-1} higher in $\Delta H_{0\mathrm{K}}$ than the lowest-lying rotamer, *cis*.[32] As we are aware of no other study that has reported this rotamer, it is unclear whether the rotamer exists or whether its identification is an artifact of the DFT functional used, B3LYP. If the rotamer is a stationary point, then is it energetically accessible? This question is difficult to answer, as the barrier to convert from this third rotamer to the others is unknown.

3. What is the origin of a 38.4 kcal mol^{-1} disagreement over the isomerization barrier between sulfurous acid and the sulfonic acid (Figure 1c) isomer? Voegele, Liedl, and coworkers computed an electronic energy barrier of 101.1 kcal mol^{-1} to form sulfonic acid from sulfurous acid using the Gaussian-3 (G3) method.[65] In contrast, Mousavipour *et al.* computed a 62.7 kcal mol^{-1} ΔH barrier at an unspecified temperature for this reaction at

CCSD(T)//MP2/aug-cc-pVTZ.[70] A discrepancy this large casts doubt on the accuracy of previous studies.

4. What is the anharmonic infrared spectrum of sulfurous acid? We are aware of only two relevant publications. The first is a report of the anharmonic $-$OH stretch frequencies for the lowest energy complexes of *cis* and *trans*-sulfurous acids with water at MP2/aug-cc-pVDZ.[73] The frequencies of other modes are not provided, and this study does not report the frequencies of isolated sulfurous acid. The second publication reports scaled harmonic vibrational frequencies at MP2/aug-cc-pVTZ for *cis*-sulfurous acid.[24] As such, these results provide no information about resonances, nor did the authors state the symmetry of the normal modes. Further, both studies used MP2 with a correlation consistent basis set lacking tight d functions. It is unclear what the error due to the choice of method will be. The neglect of tight d functions commonly causes errors in harmonic frequencies of over 20 wavenumbers, compared to the basis sets with tight d functions.[72,74,75] The MP2 approximation may contribute additional errors.

In this research, we answer these questions by studying the surface of sulfurous acid at the highest levels of *ab initio* theory to date. Herein, we provide a comprehensive analysis of the entire SO_2+H_2O surface including highly acccurate energetics of all reactions. We identify new stationary points on the surface and compute zero kelvin enthalpies for all stationary points. The following computations have led us to identify previously unrecognized problems in the theoretical literature. We then report, for the first time, true anharmonic predictions for the infrared spectra of the relevant conformers of sulfurous acid, as well as the sulfonic acid isomer.

II. THEORETICAL METHODS

A. Geometries

The geometries of all species studied were optimized using explicitly correlated coupled cluster theory with single, double, and perturbative triple excitations [CCSD(T)-F12b][76,77] using the cc-pVTZ-F12 basis sets designed for use with explicitly correlated methods.[78] These include the tight d functions for sulfur, so we henceforth refer to this as the cc-pV(T+d)Z-F12 basis set for clarity. All geometries were optimized by finite difference of energies from MOLPRO 2010.1

and MOLPRO 2015.1.[79] While the majority of optimizations were driven by MOLPRO 2010.1, some optimizations were driven by PSI4 1.2 to parallelize the energy computations across multiple computers.[80] For all these computations, the core electrons occupying the 1*s* shell of oxygen atoms and the 1*s*, 2*s*, and 2*p* shells of sulfur atoms were not correlated. This constitutes the "frozen-core" approximation. The Hartree–Fock densities were converged to within 10^{-12} and the coupled cluster energies were converged to within 10^{-12} Hartree. The internal coordinates of each geometry were converged to a root-mean-square force of at most 2×10^{-7} Hartree Bohr^{-1} using the four-point gradient in both programs. For structures of H_2SO_3 for which anharmonic frequencies are predicted, we further optimized the geometries to within 10^{-8} Hartree Bohr^{-1} to minimize errors in the anharmonic calculations.

B. Harmonic Vibrational Frequencies and Characterization of Stationary Points

Harmonic vibrational frequencies were then computed by finite difference of energies for each stationary point at the same level of theory used for the optimization. All reported transition states have a single imaginary frequency, while the other stationary points have all real frequencies. The optimized geometries and vibrational frequencies are reported in the Supplementary Information. For all transition states, the minima they connected were confirmed by an intrinsic reaction coordinate (IRC) computation using the Gonzalez–Schlegel algorithm[81] in a developer version of PSI4 1.4.[80] For most transition states, the electronic energy was computed using density-fitted B3LYP/cc-pV(T+d)Z and a grid of 590 spherical points and 99 radial points. For the second dissociation transition state from *cis*-sulfurous acid and the sulfonic acid dissociation transition state, density-fitted MP2/cc-pV(T+d)Z was used instead,[82] as the IRCs attempted with B3LYP terminated prematurely. All geometries along the IRC were optimized to a root-mean-square force less than 10^{-6} Hartree Bohr^{-1}. All IRC trajectories are included in the Supplementary Information.

C. Energies

Convergence of the relative electronic energies with respect to method and basis set was monitored by the focal point approach (FPA) of Allen and coworkers.[83–86] For each species, the energy was computed using correlation-consistent basis sets up to cc-pV(5+d)Z[71,87–89] at the CCSD(T) level. The energy was then extrapolated to the complete basis set (CBS) limit.[90,91] As such, F12

computations were not used for the energy computation. This energy, relative to that of the reactants, is $\Delta E_{\text{e,CBS}}$. To obtain the final energy, ΔE, the following corrections, relative to water and SO_2, were added to $\Delta E_{\text{e,CBS}}$:

1. To estimate the contribution of full triple excitations and perturbative quadruple excitations, the following correction was computed using the cc-pV(D+d)Z and cc-pV(T+d)Z basis sets with coupled cluster methods implemented in CFOUR 2.0[92] using the NCC module of Matthews:

$$\Delta_{\text{T(Q)}} = (\Delta E_{\text{CCSDT(Q)/DZ}} - \Delta E_{\text{CCSDT/DZ}}) + (\Delta E_{\text{CCSDT/TZ}} - \Delta E_{\text{CCSD(T)/TZ}}).$$

2. To estimate the effect of the frozen core approximation, the energy was corrected with the difference between energies with and without the frozen core approximation at the CCSD(T)/cc-pwCVQZ level[89,93] using MOLPRO 2010.1:[79]

$$\Delta_{\text{CORE}} = \Delta E_{\text{AE-CCSD(T)}} - \Delta E_{\text{CCSD(T)}}.$$

   where AE denotes an all-electron computation, that is, one without the frozen core approximation.

3. To estimate relativistic effects, a scalar correction was computed at the all-electron CCSD(T)/cc-pwCVTZ level[89,93] in CFOUR 2.0. The correction was obtained using direct perturbation theory at second order in c^{-1} (DPT2) and includes the Darwin-term and one-electron and two-electron mass-velocity terms:[94,95]

$$\Delta_{\text{REL}} = \Delta E_{\text{AE-CCSD(T)/DPT2}} - \Delta E_{\text{AE-CCSD(T)}}.$$

4. To estimate the effect of the Born–Oppenheimer approximation, the diagonal Born–Oppenheimer correction[96,97] was computed using the cc-pV(T+d)Z[71,87,88] basis set, at the RHF level in CFOUR 2.0.[92] In this correction, $\hat{T}_n$ is the nuclear kinetic energy operator and $\Psi_e(r;R)$ is the electronic wavefunction with parametric dependence on nuclear coordinates:

$$\Delta_{\text{DBOC}} = \langle \Psi_e(r;R) | \hat{T}_n | \Psi_e(r;R) \rangle \, .$$

To obtain the final enthalpy at zero kelvin, $\Delta H_{0\mathrm{K}}$, relative to the $SO_2 + H_2O$ reactants, the difference in harmonic zero-point vibrational energy (ZPVE) between the relevant species and *cis*-sulfurous acid was added. The harmonic ZPVE was calculated using the harmonic vibrational frequencies described in Section II B. Thus, the final enthalpy can be written as:

$$\Delta H_{0\mathrm{K}} = \Delta E_{\mathrm{e,CBS}} + \Delta_{\mathrm{T(Q)}} + \Delta_{\mathrm{CORE}} + \Delta_{\mathrm{REL}} + \Delta_{\mathrm{DBOC}} + \Delta_{\mathrm{ZPVE}} \tag{1}$$

D. Multireference Methods

One of the transition states considered in this work, which connects *cis*-sulfurous acid and sulfonic acid, exhibited multireference character. CASSCF computations performed as multireference diagnostics showed a natural orbital occupation number of approximately 0.5 for the S−H σ^* spatial orbital and approximately 1.5 for the S−H σ spatial orbital. The determinants with these orbitals occupied had weights of 0.709 and 0.249, respectively. Other orbitals had nearly integer natural spatial orbital occupation numbers of at worst 0.03 for virtual orbitals and 1.97 for occupied orbitals. All other determinants had a weight of 0.004 or smaller. Those natural orbital occupation numbers and weights are comparable to those of sulfonic acid. Our focal point analysis, described in Section II C and included in the supporting information, showed smooth convergence of the electronic energy of sulfonic acid. This indicates that sulfonic acid is single reference. By comparison, we conclude that the other configurations do not contribute to the multireference character of the transition state.

The geometry of the transition state between *cis*-sulfurous acid and sulfonic acid was reoptimized at MRCISD+Q/CAS(2,2)/cc-pV(T+d)Z[98,99] using MOLPRO 2010.1[79]. The same "frozen core" approximation described in Section II C was used for the multireference computations as well. The Davidson cluster correction was computed with standard reference energies and the coefficient of the fixed reference function. The vibrational frequencies were also recomputed about the multireference optimized geometry at the same level of theory.

E. Anharmonic Frequencies

For *cis*-sulfurous acid, *trans*-sulfurous acid, and sulfonic acid, the fourth derivative tensor of energy with respect to nuclear positions, a quartic force field, was computed by finite difference of

energies in internal coordinates using step sizes of 0.01 Å for bond lengths, 0.01 radians for bond angle, and 0.02 radians for torsional angles. The energies were evaluated with CCSD(T)-F12b/cc-pV(T+d)Z-F12 by MOLPRO 2010.1 and MOLPRO 2015.1.[79] The INTDER program[100] was used to transform displacements from the internal coordinates to normal coordinates using the coordinate transformation formulas of references 101 and 102. Once the force constants were obtained, a VPT2 computation[103–105] was performed to determine spectroscopic constants, anharmonic frequencies, and anharmonic ZPVE.

Strong interactions were deperturbed and treated variationally, in the so-called VPT2+K procedure.[106] We detected resonances as follows. We determined Fermi resonances by considering every pair of harmonic one quantum mode and harmonic two quanta mode that were within 200 cm^{-1} of each other. We then calculated the Martin diagnostic,[106] the difference between the perturbative correction and the variational correction, for the resulting 2-×-2 matrix. If the difference exceeded 1 cm^{-1}, the resonance was a candidate for an effective Hamiltonian treatment. For each resonance, an effective Hamiltonian matrix was constructed including both of the states found to be resonant by the Martin diagnostic, in addition to any states which are further in resonance with a state already in the matrix. Matrices larger than 2-×-2 are called polyads. Diagonal elements were populated with the VPT2 vibrational frequencies, after removing resonance denominators. These include but are not limited to resonances identified by the Martin diagnostic. For example, for *cis*-sulfurous acid, ν_{11} is in Fermi resonance with the $\nu_6 + \nu_{12}$ combination band, so the corresponding resonance denominator must be removed. However, ν_6 resonates with $2\nu_{12}$, which in turn resonates with ν_7. So to treat this resonance, the $3\nu_{12}$ and $\nu_7 + \nu_{12}$ states must be included in the effective Hamiltonian, and the denominators corresponding to the combination of modes 11, 7, and 12 must also be removed. Lastly, off-diagonal elements were populated with the appropriate constants, including the so-called "+K" terms.[105]

Infrared intensities were computed from dipole derivatives taken from a harmonic CCSD(T)/cc-pV(T+d)Z computation. The dipole derivatives were computed in the normal mode basis of the CCSD(T)/cc-pV(T+d)Z and assumed to have the same values in the normal mode basis of the CCSD(T)-F12b/cc-pV(T+d)Z-F12 computation. The final intensities used are the harmonic intensities scaled by the ratio of the anharmonic to harmonic frequencies:

$$I_\nu = I_\omega \frac{\omega_{\text{(T+d)Z}}}{\nu_{\text{(T+d)Z-F12}}}$$

For states obtained from an effective Hamiltonian, the intensity of a given vibrational transition must be further multiplied by the square of the weight of the harmonic oscillator fundamental normal mode. We report all fundamental frequencies, as well as the frequencies of any combination bands and overtones that achieve an intensity of at least 1 km mol^{-1} due to the intensity borrowing enabled by the effective Hamiltonian treatment.

The quartic force fields are reported in the Supporting Information, along with the computations performed for resonance diagnostics as well as the anharmonic ZPVE corrections.

III. RESULTS AND DISCUSSION

We structure the presentation of our results as follows: First, we present our study of the stationary points on the potential energy surface. Due to the extent of the surface, we further divide this into our investigations of the relatively well-studied *cis* and *trans* rotamers, of the mysterious third rotamer reported by Li, Bu, and coworkers,[32] of sulfonic acid and the contradictory reports of its energetics, and of the dissociation pathway. In each section, we present our geometry, compare it to previous reported geometries and explain discrepancies in the literature. We do the same for the energy afterwards. We thus assemble, piece by piece, the potential energy shown in Figure 2. After the stationary points of the surface are fully discussed, we discuss the predicted anharmonic spectra of the key minima on the surface.

When comparing our results to those of previous papers, we compare to all papers that, to our knowledge, report geometries or energies for the species studied, with two exceptions. We do not compare to results at non-correlated levels of theory, such as in references 42 and 44, nor do we compare to results that we have attempted to reproduce but not been successful. These include reference 68 as well as the results with the cc-pV(T+d)Z basis set from reference 107.

Lastly, we shall refer to sulfurous acid as if it has a central S=O covalent bond, following the convention of the majority of the scientific literature. Previous work concluded on the basis of natural bonding orbital analyses that the bond was better regarded as an $S^{+}-O^{-}$ ionic bond.[108] Investigation into which Lewis structure best describes the molecule is beyond the scope of the present work.

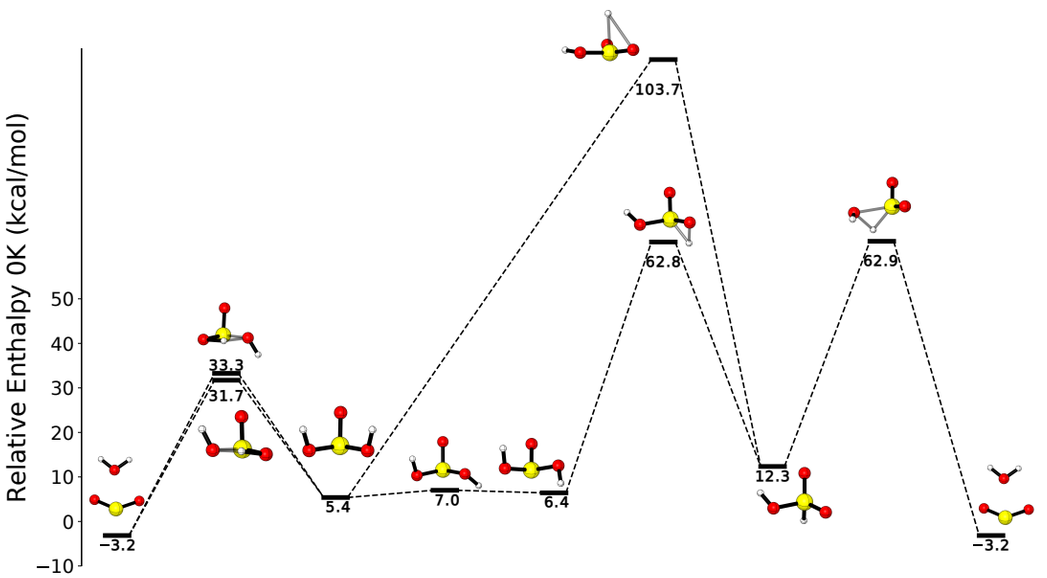

FIG. 2: The potential energy surface for sulfurous and sulfonic acids computed at FPA//CCSD(T)-F12b/cc-pV(T+d)Z-F12 level of theory. Enthalpies are in kcal mol^{-1} and relative to the separated H_2O and SO_2 reactants. From left to right, the figure depicts the dissociated structure, the *cis* and *trans* rotamers of sulfurous acid, sulfonic acid, and finally the dissociated structure again.

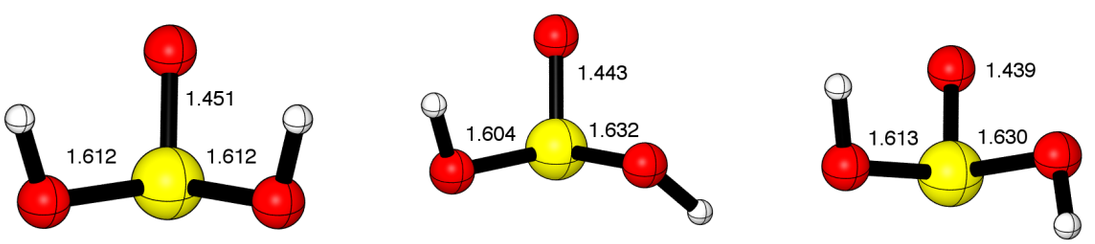

(a) *cis*-sulfurous acid

(b) *cis-trans* isomerization transition state

(c) *trans*-sulfurous acid

FIG. 3: The geometries of *cis*-sulfurous acid (a), the transition state between the rotamers (b), and *trans*-sulfurous acid (c). All geometries were optimized at the CCSD(T)-F12b/cc-pV(T+d)Z-F12 level of theory. Distances are in Å.

TABLE I: Select internal coordinates of *cis*-sulfurous acid computed by this study and previous research. Entries are ordered by method, and then from least to most complete basis set. All distances are in angstroms, and all bond angles are in degrees.

Ref.	Method	Basis Set	S=O	S−O	H−O−S
This work	CCSD(T)-F12b	cc-pV(T+d)Z-F12	1.451	1.612	107.9
69	MPW1K	M3GS	1.438	1.592	109.4
65	B3LYP	6-31+G(d)	1.481	1.666	109.0
51	B3LYP	6-311+G(d,p)	1.474	1.664	109.7
107	B3LYP	aug-cc-pVTZ	1.469	1.647	
51	B3LYP	6-311+G(d,p), +G(3df) on sulfur	1.456	1.631	109.3
48	MP2	6-31G(d)	1.47	1.66	
47	MP2	6-31G(d)	1.474	1.654	107.3
70	MP2	aug-cc-pVTZ	1.469	1.635	106.8
49	MP2	6-311++G(3df,2p)	1.454	1.619	107.9

A. Potential Energy Surface

1. Cis and Trans Sulfurous Acid Rotamers: Geometries

cis-sulfurous acid (Figure 3a) has C_s symmetry, and we find that it has a central S=O double bond 1.451 Å long and two symmetry-equivalent S−O bonds each 1.612 Å long. The O−S−O angle is 100.6°. Each O=S−O angle is 105.6°. Finally, the H−O−S angles are 107.9°.

We compare our geometry for *cis*-sulfurous acid with those of previous publications in Table I. Previous reports of the S=O bond length computed by MP2 and B3LYP have been longer than our bond length by up to 0.03 Å. For both methods, this error decreases as the size of the basis set increases. Values computed with the largest basis set prior to this study, 6-311++G(3df,2p), disagree with our high level result only by 0.003 Å, despite treating electron correlation only at the MP2 level. We thus attribute the majority of the disagreements over this bond length in the literature primarily to basis set effects. Basis set effects do not explain the MPW1K/M3GS computation of reference 69, which is an outlier. To further validate the reliability of our data, we observe that the experimental equilibrium distance of the S=O double bond of SO is 1.481 Å,[109] and the experimental equilibrium distance of each of the the SO_2 double bonds is 1.431 Å.[110,111] Our value of 1.451 Å is well within the range expected of the S=O double bond.

The length of the two symmetry-equivalent S−O bonds displays a similar trend. Table I shows

TABLE II: Select internal coordinates of *trans*-sulfurous acid computed by this study and previous research. Entries are ordered by method, and then from least to most complete basis set. All distances are in angstroms, and all bond angles are in degrees.

Ref.	Method	Basis Set	S=O	*syn* S−O	*anti* S−O	*syn* H−O−S	*anti* H−O−S
This work	CCSD(T)-F12b	cc-pV(T+d)Z-F12	1.439	1.613	1.630	108.3	108.8
66	M06-2X	6-31G(d,p)	1.455	1.635	1.647	108.0	108.9
51	B3LYP	6-311+G(d,p)	1.460	1.667	1.686	109.7	109.5
107	B3LYP	aug-cc-pVTZ	1.457		1.667		
51	B3LYP	6-311+G(d,p), +G(3df) on sulfur	1.443	1.632	1.652	109.5	109.2
49	MP2	6-311++G(3df,2p)	1.442	1.620	1.639	108.3	108.6

that previously reported bond lengths were up to 0.05 Å longer than our S−O bonds and converge to our value as basis set increases. Even MP2 correlation provides bond lengths close to our high level bond lengths, given a sufficiently large basis set, as in reference 49. The small disagreement indicates that a yet more precise theoretical treatment is unlikely to change the bond length significantly from our values.

The only other geometric parameter for which significant differences were observed is the H−O−S angle, where MP2 agrees excellently with our high-level computations, but B3LYP predicts an angle that is 1-2 degrees too large. We also note that MPW1K/M3GS is unusual, being the only method to underpredict bond lengths.[69]

Because the *trans* rotamer does not have symmetry, it has more inequivalent internal coordinates. For this rotamer (Figure 3c), one of the O−H groups (the *syn* group) points in the same direction as the S=O bond, and the other O−H group (the *anti* group) points in the opposite direction. Compared to the *cis* rotamer of sulfurous acid, the S=O bond has contracted from 1.451 Å to 1.439 Å in the *trans* rotamer. Of the S−O bonds, the *syn* is at 1.613 Å, quite similar to the bond length of its counterpart in the *cis* rotamer. Meanwhile, the *anti* S−O bond has lengthened from 1.612 to 1.630 Å. The O−S−O angle has contracted to 98.9°, and the *cis* and *trans* O=S−O angles are respectively 107.6 and 102.4°. Each S−O−H angle has expanded, respectively moving to 108.3 and 108.8°.

The geometry of the *trans* rotamer has been reported, from theory, four times.[49,51,66,107] The comparison between our geometry and previously reported geometries, shown in Table II, is anal-

ogous to the comparison for the *cis* rotamer from Table I. S=O and S−O show errors with small basis sets, with S−O lengths being especially basis-set sensitive. MP2 with a large basis set give bond lengths within 0.01 Å of our values, and B3LYP computes too large of an H−O−S angle with any basis set considered. Lastly, M06-2X/6-31G(d,p) has a more compact geometry for this rotamer than B3LYP paired with multiple basis sets. It is unclear from this comparison how M06-2X would perform with other basis sets.

Next, we report the geometry of the transition state for *cis-trans* isomerization (Figure 3b) for the first time. The S=O bond is 1.443 Å, intermediate between the two rotamers. The *syn* S−O bond is 1.604 Å long, nearly 0.01 Å shorter than either of the equilibrium structures, and the *anti* S−O bond is 1.632 Å long, which is only marginally longer than in the *trans* minima.

On the basis of our computed geometries, we reject the claim of Li, Bu, and coworkers that both the existence and the energetic ordering of distinct *cis* and *trans* H_2SO_3 rotamers should be understood in terms of hydrogen bonding between the SOH hydrogens and the S=O oxygen.[32] First, the evidence for hydrogen bonding is uncompelling. The angle between the proposed hydrogen bond acceptor, the hydrogen, and the hydrogen bond donor is much closer to 90° than the ideal 180° of a strong and indisputable hydrogen bond. Second, such a view cannot rationalize the differences in the geometries of these rotamers. The model of reference 32 would predict that when one of the OH bonds rotates *anti* to the S=O, a hydrogen bond breaks. The hydrogen bond would decrease the distance between the hydrogen and the acceptor, so losing the bond should cause both S=O and S−O bond distances to increase. While this rotation causes the S−O bond length to expand, the S=O bond length *contracts*. Third, we also observed along the intrinsic reaction coordinate path (IRC) that as the *anti* OH group rotates, the *syn* OH group temporarily rotates in the same direction before reverting back. We observe that at the point of greatest twisting, one of the two *syn* oxygen lone pairs are in an orientation promoting overlap with both lone pairs of the *anti* oxygen. Hydrogen bonding cannot explain this.

We instead explain the structure and the energetics of the rotamers with hyperconjugation. We begin with the rotation. Second order perturbative analysis of natural bonding orbitals[112] shows a strong interaction between each S−O antibonding orbital and a lone pair on the other singly bound oxygen. While the *anti* group rotates and its lone pair moves, the *syn* oxygen twists to partially hyperconjugate with the *anti* S−O antibonding orbital but partially to hyperconjugate with the S=O antibonding orbital. The hyperconjugation is restored, although in a weaker form, when the

anti oxygen completes its rotation, moving its lone pair back into position. As for energy, the second order perturbative analysis also reveals a hyperconjugation interaction between the O−H antibonding orbitals and the S=O. This interaction will be stronger when both O−H groups are in position to hyperconjugate, so we may predict the *cis* rotamer to be energetically favored. Further, this hyperconjugation interaction would cause the oxygen to lose electron density, leading to a weaker electrostatic interaction and thus the observed slight lengthening of the S=O bond in the *cis* rotamer.

2. Cis and Trans Sulfurous Acid Rotamers: Energetics

Energies of the *cis* rotamer have been reported many times. Some reports include the energy of *cis*-sulfurous acid relative to isolated SO_2 and H_2O, but not the energy relative to the $SO_2 \cdots H_2O$ complex, and vice versa. In this section, we only discuss the energies relative to isolated SO_2 and H_2O, deferring comparison with the complex to section III A 5.

We find an electronic dissociation energy of 2.7 kcal mol^{-1} and an enthalpy of 5.4 kcal mol^{-1}. Previous papers have reported a wide range for both numbers, as shown in Table V. Reported electronic energies have varied over an 8 kcal mol^{-1} range, from 1.4 to 9.4 kcal mol^{-1}. Coupled cluster predictions have been within the narrower range of 1.4 to 3.1 kcal mol^{-1}. For enthalpy, computations have varied from 3.1 to 12.9 kcal mol^{-1}, a range of almost 10 kcal mol^{-1}.

To demonstrate that the relative energies for the sulfurous acid rotamers are converged, we present an incremented focal point table for the *cis*-sulfurous acid rotamer in Table III. The tables for the *trans*-sulfurous acid rotamer and the transition state between the two rotamers are similar. The energy changes only marginally in response to increasing our level of electron correlation or to enlarging the basis set, so we conclude our relative energies are reliable to within 1 kcal mol^{-1}. Energy differences between individual rotamers are even tighter, with a post-CCSD(T) correction of only -0.02 kcal mol^{-1}, as demonstrated in Table IV. However, it is less clear why we see so much scatter in previous results. We attribute the variance to three causes:

1. Computing the energy with a smaller basis set can introduce errors of up to 8 kcal mol^{-1}. Table V shows the worst reported perfomer as QCISD(T)/6-311++G(d,p)//MP2/6-31G(d),[48] which disagrees with our ΔE_e by 6.4 kcal mol^{-1}. To analyze the disagreement, we performed a QCISD(T) computation with varying basis sets on the MP2/6-31G(d) geometry.

TABLE III: Incremented focal point table for the enthalpy difference between *cis*-sulfurous acid and the separated SO_2 plus H_2O reactants. Energies are computed as described in Section II C, using $\Delta H_{0K} = (\Delta E_{e,CBS} + \Delta_{T(Q)}) + \Delta_{CORE} + \Delta_{REL} + \Delta_{DBOC} + \Delta_{ZPVE}$. All energies are in kcal mol^{-1}. Values in square brackets for a specific basis set are additive corrections. See the Supporting Information for more extensive energy benchmarks.

Basis Set	ΔE_e HF	+δ MP2	+δ CCSD	+δ CCSD(T)	+δ CCSDT	+δ CCSDT(Q)	ΔE_e Net
cc-pV(D+d)Z	−3.32	+12.47	−4.28	+1.93	+0.01	+0.56	[+7.37]
cc-pV(T+d)Z	−3.67	+8.43	−3.87	+1.69	−0.03	[+0.56]	[+3.10]
cc-pV(Q+d)Z	−3.03	+7.66	−4.41	+1.64	[−0.03]	[+0.56]	[+2.39]
cc-pV(5+d)Z	−2.52	+7.44	−4.65	+1.63	[−0.03]	[+0.56]	[+2.42]
CBS	[−2.17]	[+7.21]	[−4.90]	[+1.61]	[−0.03]	[+0.56]	**[2.28]**

$$\Delta H_{0K} = 2.28 + 0.18 + 0.24 - 0.02 + 2.70 = \mathbf{5.38}$$

TABLE IV: Incremented focal point table for the enthalpy difference between *trans*-sulfurous acid and *cis*-sulfurous acid. Energies are computed as described in Section II C, using $\Delta H_{0K} = (\Delta E_{e,CBS} + \Delta_{T(Q)}) + \Delta_{CORE} + \Delta_{REL} + \Delta_{DBOC} + \Delta_{ZPVE}$. All energies are in kcal mol^{-1}. Values in square brackets for a specific basis set are additive corrections. See the Supporting Information for more extensive energy benchmarks.

Basis Set	ΔE_e HF	+δ MP2	+δ CCSD	+δ CCSD(T)	+δ CCSDT	+δ CCSDT(Q)	ΔE_e Net
cc-pV(D+d)Z	2.01	−0.67	+0.22	−0.04	−0.03	+0.00	[+1.49]
cc-pV(T+d)Z	1.73	−0.72	+0.23	−0.09	−0.02	[+0.00]	[+1.13]
cc-pV(Q+d)Z	1.61	−0.78	+0.26	−0.11	[−0.02]	[+0.00]	[+0.96]
cc-pV(5+d)Z	1.54	−0.80	+0.29	−0.12	[−0.02]	[+0.00]	[+0.89]
CBS	[1.50]	[−0.82]	[+0.31]	[−0.13]	[−0.02]	[+0.00]	**[0.84]**

$$\Delta H_{0K} = 0.84 + 0.00 + 0.02 + 0.00 + 0.19 = \mathbf{1.05}$$

We reproduced the previously reported energy to within 0.02 kcal mol^{-1} using the original 6-311++G(d,p) basis set. Using the larger 6-311++G(3df,p) and cc-pV(5+d)Z basis sets reduce ΔE_e from 9.4 to 5.0 and 1.3 kcal mol^{-1}, respectively. This comparison against reference 48 shows that basis set error can reach 8.1 kcal mol^{-1}.

2. Computing the energy at a less than optimal geometry can introduce error over 1.5 kcal mol^{-1}. Previous work[50] reported an electronic energy difference of 7.1 kcal mol^{-1} for MP2/aug-cc-pVDZ. We reproduced this number. However, performing MP2/aug-cc-pVDZ at our geometries yielded an electronic energy difference of 5.5 kcal mol^{-1}. This is a geometry error of 1.6 kcal mol^{-1}. See Table I for typical errors in *cis*-sulfurous geometries.

TABLE V: Energies of *cis*-sulfurous acid relative to the separated $SO_2 + H_2O$ reactants computed in this research and in previous works. Entries are ordered by method, and then from least to most complete basis set. ΔE energies have no zero-point correction. All energies are in kcal mol^{-1}.

Ref.	E_e Method	Geometry/ZPVE Method	ΔE	ΔH_{0K}
This work	FPA	CCSD(T)-F12b/cc-pV(T+d)Z-F12b	2.7	5.4
50	B3LYP/6-31+G(d)	B3LYP/6-31+G(d)	1.7	
30	B3LYP/6-311+G(2df,2p)	B3LYP/6-311+G(2df,2p)	2.5	4.9
30	B3LYP/6-311++G(3df,3pd)	B3LYP/6-311++G(3df,3pd)	3.3	5.8
50	MP2/aug-cc-pVDZ	MP2/aug-cc-pVDZ	7.1	
50	MP2/aug-cc-pVTZ	MP2/aug-cc-pVTZ	4.7	
48	MP4SDQ/6-31G(d)	MP2/6-31G(d)	2.1	5.5
48	MP4SDQ/6-311++G(d,p)	MP2/6-31G(d)	8.8	12.2
48	QCISD(T)/6-31G(d)	MP2/6-31G(d)	3.2	6.7
48	QCISD(T)/6-311++G(d,p)	MP2/6-31G(d)	9.4	12.9
46,47	G2		2.7	5.8
30	CCSD/6-311+G(2df,2p)	B3LYP/6-311+G(2df,2p)	2.3	4.7
30	CCSD/6-311++G(3df,3pd)	B3LYP/6-311++G(3df,3pd)	3.1	5.6
31,50	CCSD(T)/aug-cc-pVDZ	MP2/aug-cc-pVDZ	1.8	
33	CCSD(T)/aug-cc-pVDZ	MP2/aug-cc-pVDZ		4.5
107	CCSD(T)/aug-cc-pVTZ	B3LYP/aug-cc-pVTZ	1.4	3.9
35	CCSD(T)/CBS	B3LYP/cc-pV(T+d)Z		3.1

3. Our energy computation includes additive corrections for the frozen core approximation, relativistic effects, and most importantly, electron correlation beyond perturbative triple excitations. These individually small corrections sum to about a 1 kcal mol^{-1} increase in our computed ΔE_e and have not been accounted for in previous studies.

As for the enthalpy, we find that harmonic zero-point vibrational energy lowers the SO_2 and H_2O reactants by an additional 2.7 kcal mol^{-1}. Previous studies give between 2.4 and 3.5 kcal mol^{-1} for this quantity, which is a large relative uncertainty. Yet again, we attribute this to basis set deficiency. Given the variation seen in geometries, shown in Tables I and II, we expect variation in normal mode frequencies and thus the zero-point energy.

We find that the energy difference between the *cis* and *trans* rotamers is 0.9 kcal mol^{-1} in electronic energy and 1.1 kcal mol^{-1} in ΔH_{0K}. This is within the narrow range of electronic energy reported by previous studies, shown in Table VI.

Lastly, the transition state between the *cis* and *trans* rotamers has a ΔH_{0K} value of 1.6

TABLE VI: Energies of *trans*-sulfurous acid relative to *cis*-sulfurous acid computed in this work and in previous works. Entries are ordered by method, and then from least to most complete basis set. ΔE energies have no zero-point correction. All energies are in kcal mol^{-1}.

Ref.	E_e Method	Geometry/ZPVE Method	ΔE	ΔH_{0K}
This work	FPA	CCSD(T)-F12b/cc-pV(T+d)Z-F12b	0.9	1.1
107	CCSD(T)/aug-cc-pVTZ	B3LYP/aug-cc-pVTZ	0.8	0.9
51	B3LYP/6-111+G(d,p)	B3LYP/3-111+G(d,p)	0.7	0.9
51	B3LYP/6-311+G(d,p), +G(3df) on sulfur	B3LYP/6-311+G(d,p), +G(3df) on sulfur	0.5	0.8
32	B3LYP/6-311++G(3df,3pd)	B3LYP/6-311++G(3df,3pd)		0.9
32	BP86/TZ2P	B3LYP/6-311++G(3df,3pd)		0.8
1	CCSD(T)/aug-cc-pVTZ	MP2/aug-cc-pVTZ	1.0	

kcal mol^{-1} relative to the *cis* rotamer and 0.6 kcal mol^{-1} relative to the *trans* rotamer. These energies are shown in Figure 2. Hence, we expect that equilibrium is easy to achieve, and at equilibrium, the *cis* rotamer would be only slightly favored, even at low temperatures. Tunneling between the two rotamers would allow for even more rapid interconversion.

The previous value for this barrier height was the 2.4 kcal mol^{-1} CCSD(T)//MP2/aug-cc-pVTZ electronic energy of Liedl and coworkers, excluding ZPVE.[1] By comparison, the CCSD(T)/cc-pV(5+d)Z//CCSD(T)-F12b/cc-pV(T+d)Z-F12 electronic energy we compute is 1.8 kcal mol^{-1}. While it is tempting to attribute this to our improved basis set, attempts to reproduce the barrier height with the methods of Voegele gave an electronic energy barrier of 2.0 kcal mol^{-1}, not the 2.4 kcal mol^{-1} they reported, even though we could reproduce their other electronic energy computations to the reported 0.01 kcal mol^{-1} precision.

3. Third Sulfurous Acid Rotamer

We confirm the previous report that a third sulfurous acid rotamer is a minima on the electronic energy surface.[32] Li and coworkers identified the structure with B3LYP/6-311++G(3df,3pd). Even after we had optimized the rotamer at CCSD(T)-F12b with the cc-pV(D+d)Z-F12 and cc-pV(T+d)Z-F12 basis sets, attempts to optimize the structure at B3LYP/6-31+G(d) and CCSD(T)/cc-pV(D+d)Z failed. We conclude that the minimum only exists on potential energy surfaces computed with relatively large basis sets, explaining why there has only been one previous report of this rotamer.

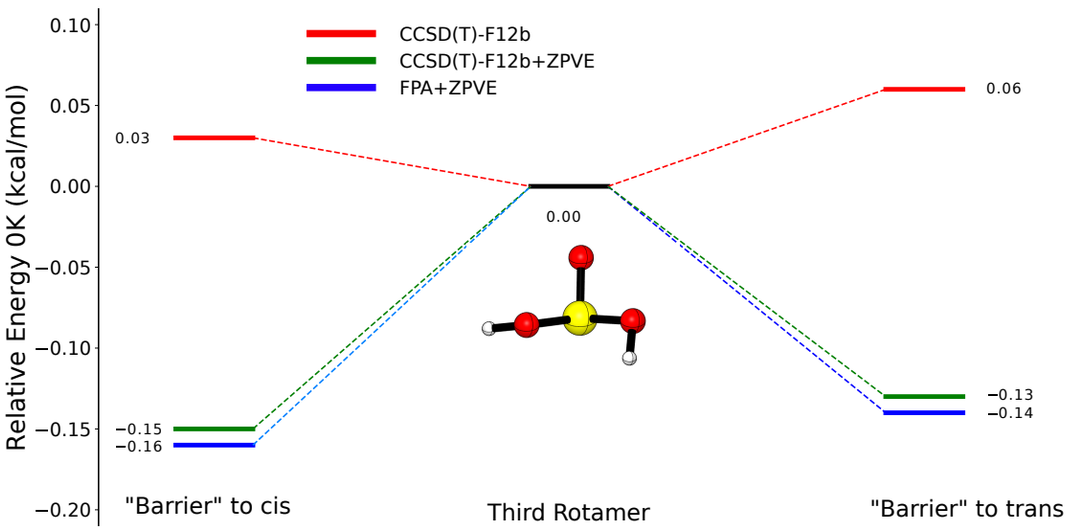

FIG. 4: The barriers to rotation from the third rotamer of sulfurous acid to the *cis* and *trans* rotamers computed in this work. At the CCSD(T)-F12b/cc-pV(T+d)Z-F12 level of theory used in the optimization, the barriers are less than 0.1 kcal mol^{-1}. Upon adding ZPVE contributions, rotation of the −OH groups into a different well is barrierless. The Focal Point Analysis (FPA) described in Section II C gives the same conclusion.

We find that although one of the O−H bonds of this rotamer is *anti* to the S=O bond, the other O−H bond is neither *syn* nor *anti* but perpendicular, i.e., sideways. The sideways S−O is unusually long at 1.641 Å and the *anti* S−O is shorter than in the *trans* structure, now at 1.614 Å rather than 1.630. The O−S−O angle has contracted to 92.7°. We find that this rotamer is 3.3 kcal mol^{-1} higher in ΔH_{0K} than the *cis* rotamer, slightly higher than the previous value of 2.8 kcal mol^{-1} computed with BP86/TZ2P//B3LYP/6-311++G(3df,3pd).[32]

Nonetheless, this rotamer is of no physical significance. We have identified and optimized the transition states connecting this rotamer to the *cis* and *trans* rotamers. For both, we compute an activation energy of less than 0.1 kcal mol^{-1}. Because this region of the surface is so flat, upon adding ZPVE, the transition states are lower in enthalpy than the minima. Figure 4 shows this effect and that it is independent of whether the electronic energies come from CCSD(T)-F12b method used for optimizations or the Focal Point approach used for final energies at the optimized geometries. This small barrier explains why the "minimum" only exists on surfaces with large basis sets: the basis set incompleteness error is comparable to the activation energy. We thus

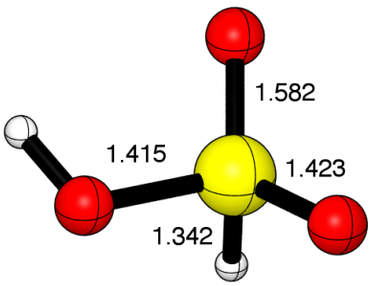

FIG. 5: The geometry of sulfonic acid, as optimized at the CCSD(T)-F12b/cc-pV(T+d)Z-F12 level of theory. Distances are in Å.

TABLE VII: Select internal coordinates of sulfonic acid computed by this study and previous research. All distances are in angstroms.

Ref.	Method	Basis Set	S−H (Å)	*syn* S−O (Å)	*anti* S−O (Å)	S=O (Å)
This work	CCSD(T)-F12b	cc-pV(T+d)Z-F12	1.342	1.415	1.423	1.582
49	MP2	6-311++G(3df,2p)	1.339	1.419	1.428	1.588
70	MP2	aug-cc-pVTZ	1.346	1.435	1.444	1.606
65	B3LYP	6-31+G(d)	1.358	1.449	1.458	1.637

interpret this "minimum" as merely a very flat region of the potential energy surface.

4. Sulfonic Acid

Although several authors have reported sulfonic acid (Figure 5) previously,[42,44,46,49,65,69,70] only three have provided information about the geometry computed at correlated levels of theory.[49,65,70]

We find that the hydrogen bound to the sulfur of sulfonic acid has a bond length of 1.342 Å. The central sulfur is bound to three oxygens. One oxygen, with S−O bond length of 1.582 Å, carries a proton. The two oxygens have S=O double bonds of length 1.415 and 1.423 Å. The longer S=O bond is *syn* to the O−H bond.

Table VII shows that the worst agreement for the S−H length we computed is with B3LYP/6-31+G(d), which predicts a 0.016 Å longer bond. Disagreements for the remaining S−O bond lengths are dominated by basis set effects. Merely neglecting tight d functions can cause errors on the order of 0.02 Å in bond lengths compared to our values that become an order of magnitude smaller upon using a larger basis set.

We have identified *two* transition states corresponding to isomerization to sulfonic acid from sulfurous acid. The first is isomerization from the *cis* rotamer (*cis*-sulfonic transition state), and the second is isomerization from the *trans* rotamer (*trans*-sulfonic transition state). The *cis*-sulfonic transition state was reported by Voegele, Liedl and coworkers,[65] and the *trans*-sulfonic transition state was reported by Mousavipour *et al.*[70] Neither paper recognized the existence of multiple sulfurous acid rotamers. Accordingly, the explanation for the 40 kcal mol^{-1} disparity for the sulfurous-sulfonic activation energies between the two papers is that the activation energies assume different transition states. We note that Mousavipour *et al.* reported performing IRCs to verify the connectivity of all of their transition states, but the transition state that they reported does not lead to the rotamer that they reported. We further observe that the *cis*-sulfonic transition state has multiconfigurational character in the S-H σ and σ^* bonding orbitals. The multireference diagnostics are discussed in greater detail in Section II D and the Supporting Information. Accordingly, geometries and energies for this species will be less accurate.

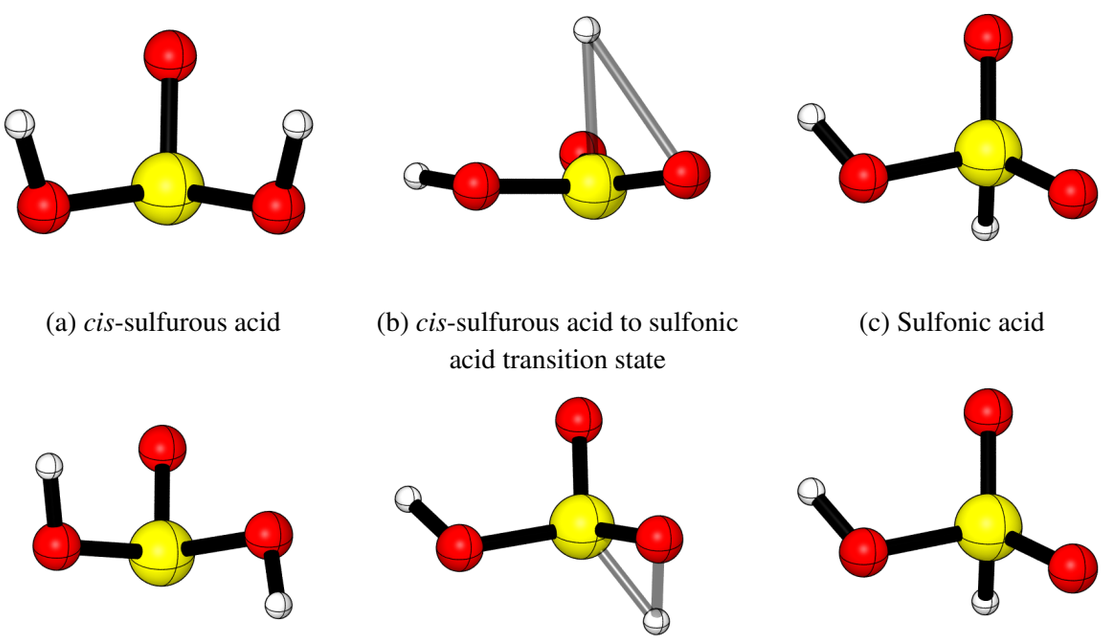

(a) *cis*-sulfurous acid

(b) *cis*-sulfurous acid to sulfonic acid transition state

(c) Sulfonic acid

(d) *trans*-sulfurous acid

(e) *trans*-sulfurous acid to sulfonic acid transition state

(f) Sulfonic acid

FIG. 6: The stationary points along the paths connecting sulfonic acid to the *cis*-sulfurous acid and *trans*-sulfurous acid rotamers. The geometry of b was optimized at MRCI+Q/CAS(2,2)/cc-pV(T+d)Z. All other species in this figure were optimized at CCSD(T)-F12b/cc-pV(T+d)Z-F12.

To form sulfonic acid (Figure 6c) from *cis*-sulfurous acid (Figure 6a), the proton that will remain on the oxygen twists backwards, going past the S=O bond. After this, the reactive proton detaches from the oxygen, and the rest of the molecule becomes planar. We are now at the transition state, Figure 6b. The moving proton hovers above the sulfur at a distance between 1.7 and 1.9 Å. The resulting geometry resembles a trigonal bipyramidal geometry from VSEPR theory, with one of the axial "atoms" now a lone pair on oxygen. The sulfur and reactive proton approach and bond while the oxygens bend in the opposite direction, restoring the tetrahedral geometry of Figure 6b.

The pathway from *trans*-sulfurous acid (Figure 6d) to sulfonic acid (Figure 6f) is much simpler. In concert, the two protons twist backwards around their respective S−O bonds, and the *anti* S−O contracts. The *syn* proton remains on its oxygen atom, but the *anti* proton transfers onto the sulfur. The transition state, Figure 6e, is simply a snapshot along this path.

We now turn our attention to energetics. We find that the sulfonic acid isomer is 7.1 kcal mol^{-1} in $\Delta H_{0\mathrm{K}}$ above the lowest lying sulfurous acid rotamer, *cis*-sulfurous acid. However, the energetic barriers connecting these isomers, shown in Figure 2, are large enough to prohibit conversion between sulfurous and sulfonic acids. At the level of theory described in Section II C, the activation barrier from sulfonic acid to the *cis*-sulfonic transition state is 91.4 kcal mol^{-1}, while the activation barrier to the *trans*-sulfonic transition state is 50.4 kcal mol^{-1}. For the *cis*-sulfonic transition state, the activation energy before auxiliary corrections is 104.8 kcal mol^{-1} with the focal point analysis, but 115.1 kcal mol^{-1}with MRCI+Q/CAS(2,2)/cc-pV(T+d)Z. In either case, the activation energy is much too high for this transition state to be relevant, even in comparison to the *trans*-sulfonic acid transition state. Given that the *cis*-sulfonic acid transition state requires an unusual variant of the trigonal bipyramidal geometry, which VSEPR theory says is higher in energy compared to a seesaw structure, that the *cis*-sulfonic acid transition state would be high in energy compared to the *trans*-sulfonic transition state is unsurprising. So as shown by Figure 2, isomerization of *cis*-sulfurous acid to sulfonic acid requires 40 kcal mol^{-1} less of $\Delta H_{0\mathrm{K}}$ if it proceeds by first rotating to *trans*-sulfurous acid and then isomerizing, compared to the direct path discovered by Voegele, Liedl, and coworkers. Thus, their computed rate constants for isomerization of sulfurous acid to sulfonic acid (on the order of 10^{-28} to 10^{-8} s^{-1} between 150 and 350 K) are qualitatively incorrect, being too low by several orders of magnitude.

Our findings for sulfonic acid qualitatively agree with previous predictions beyond the Hartree-Fock level of theory, with two noteworthy differences. First, the authors of reference 70 predicted a

relative $\Delta H_{298\mathrm{K}}$ of 15.1 kcal mol^{-1}, 8.0 kcal mol^{-1} larger than our predicted value. We have traced the disagreement back to the electronic energy computations. We predict 7.1 kcal mol^{-1} while they predict 14.4 kcal mol^{-1} with CCSD(T)//MP2/aug-cc-pVTZ. Simply by adding tight d functions to the basis set used in the CCSD(T) single point computation, we have reduced their value to 7.6 kcal mol^{-1}. This yet again demonstrates the importance of using a proper basis set to treat sulfur containing molecules. Further, given the sensitivity of theoretical kinetics to electronic energies, we assume there are several orders of magnitude of error in the rate constants reported in reference 70. Lastly, we note that sulfonic acid and its associated transition states all have relativistic corrections ranging from 0.69 to 1.17 kcal mol^{-1} relative to the isolated SO_2 and H_2O reactants. This large relativistic correction is difficult to interpret and warrants additional computational study.

5. Dissociation

SO_2 and H_2O form a chalcogen bonded complex[113] due to a dipole interaction between their respective central atoms. The complex is in a C_s "sandwich structure," with each monomer in a plane tilted with respect to the other monomer. This qualitatively agrees with the structure inferred from the microwave and infrared spectra of the complex.[17,18,21] However, our structure does not quantitatively agree with that determined via microwave spectroscopy.[21] On the basis of the poor comparison between experiment and older theory, Steudel and Steudel concluded that the experimental spectrum was incorrect.[56] We claim instead that the experimental and theoretical values cannot meaningfully be compared. Theoretical studies to date have determined an *equilibrium* structure of the complex, while Matsumura *et al.* calculated their structure by fitting the intermolecular coordinates to *vibrationally averaged* rotational constants. The intermolecular parameters of weakly bound complexes differ strongly between the two kinds of structures. For a theoretical study to meaningfully compare with the structure of Matsumura *et al.*, it must compute a vibrationally averaged geometry. This is outside the scope of the present work.

We identified three transition states corresponding to dissociation of a single molecule. Two of the transition states start from *cis*-sulfurous acid, while the third starts from sulfonic acid. The two *cis*-sulfurous dissociation transition states are quite similar. One OH group breaks its S−O bond while the other group strengthens its S−O bond to a S=O bond. This latter oxygen rotates its hydrogen towards the other O−H group for abstraction. The two transition states differ in the

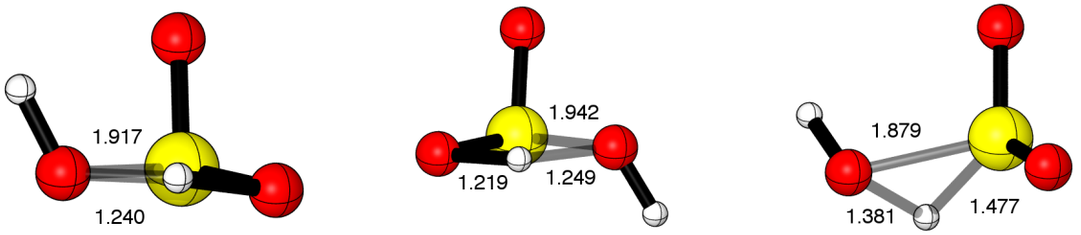

(a) Lower energy *cis*-sulfurous acid dissociation transition state

(b) Higher energy *cis*-sulfurous acid dissociation transition state

(c) Sulfonic acid dissociation transition state

FIG. 7: The geometries of the two transition states to dissociation into H_2O and SO_2 from *cis*-sulfurous acid (lower energy at a and higher energy at b), and the transition state to dissociate from sulfonic acid (c). All geometries were optimized at the CCSD(T)-F12b/cc-pV(T+d)Z-F12 level of theory. Distances are in Å.

orientation of the hydrogen already bonded to the leaving oxygen. In the more favorable transition state (Figure 7a), it is *syn* to the original S=O bond, but it is *anti* in the other transition state (Figure 7b). Most previous reports of a *cis*-sulfurous dissociation transition state were of the lower energy one,[1,30,33–35,47,48,50,65,69,70,107] except for reference 66, which reported the higher energy transition state. In the sulfonic acid transition state (Figure 7c), the S−O bond of the leaving OH group begins breaking immediately. The OH and the hydrogen bonded to the sulfur rotate towards each other until the leaving oxygen finally abstracts the proton.

We find that all three dissociation transition states lead to the "sandwich structure" complex we have discussed in this section, according to IRC computations. While the path there from the lower energy *cis*-sulfurous acid transition state (Figure 7a) is relatively straightforward, the paths from the other transition states, shown in Figure 7b and 7c, are much shallower. Much of the path is near a geometry where the SO_2 and H_2O are in roughly parallel planes. One S=O bond and one O−H bond are stacked on top of each other, but the other two bonds point in opposite directions.

High activation barriers prohibit all three dissociation reactions. The ΔH_{0K} barriers to dissociation of *cis*-sulfurous acid are 26.3 and 27.9 kcal mol^{-1}, and the barrier to sulfonic acid dissociation is 50.5 kcal mol^{-1}. The lowest *cis*-sulfurous dissociation barrier is within 3 kcal mol^{-1} of all earlier ΔH_{0K} and ΔH_{298K} with previous correlated levels of theory. Meanwhile, the sulfonic acid dissociation barrier has been refined by several kcal mol^{-1} from the 56.5 kcal mol^{-1} ΔH_{0K} of Donaldson *et al.* at MP1KW/MG3S,[69] but we remain close to the 53.4 kcal mol^{-1} computed by Voegele, Liedl, and coworkers with the G3 composite method.[65] (We caution that Liedl *et al.* re-

tained only the electronic energy terms to get a G2 energy in reference 1, and it is unclear whether they did so for G3 in reference 65.)

We find that the complex is bound by 3.2 kcal mol^{-1} $\Delta H_{0\mathrm{K}}$ and is 8.5 kcal mol^{-1} lower in $\Delta H_{0\mathrm{K}}$ than *cis*-sulfurous acid. Previous theoretical literature agrees with the binding energy to within 2.5 kcal mol^{-1}. The greatest discrepancies come from references 45 and 61, which have both conspicuously small basis sets and no accounting for triple excitation effects.

The state of the literature for the energy difference between *cis*-sulfurous acid and the complex is more intriguing. Most previous computations agree with us to within 2.5 kcal mol^{-1}, with three exceptions. The first is reference 35. The authors of reference 35 report a 6.0 kcal mol^{-1} $\Delta H_{0\mathrm{K}}$ gap at CCSD(T)/CBS//B3LYP/cc-pV(T+d)Z. However, the basis set extrapolation performed in that study is unreliable. First, the basis sets used in the extrapolation do not have tight d functions. Second, the extrapolation of reference 35 includes only the cc-pVDZ and cc-pVTZ basis sets, but our focal point tables (in the Supporting Information) demonstrate that systematic convergence with respect to basis set is not seen until after cc-pVDZ, so a proper extrapolation should exclude double zeta results for this system. The other two anomalous results are each more than 6 kcal mol^{-1} off. They were computed by reference 69 using MPW1K/MG3S and reference 66 using M06-2X/6-311++G(3df,3pd)//6-31G**. We performed single points with those functionals using cc-pV(T+d)Z on our geometries and saw similar results, so we conclude that those functionals simply perform badly for energies of the dissociated complex.

We make three caveats regarding the conclusions to be drawn from our energetic results. First, the thermochemistry computed here is for the uncatalyzed reaction. Other studies show that the dissociation reactions can be catalyzed strongly by species such as water.[1,33–35,37,47,50,69] However, we also emphasize that previous studies should not be trusted blindly, as we have shown that the theoretical methods used to study the surface without catalysts can lead to quantitatively and even qualitatively poor results. Second, the activation energies for dissociations are greater than the energies of isolated SO_2 plus H_2O, so when sulfurous and sulfonic acid dissociate, they may dissociate completely rather than form a complex. Third, a hydrogen-bonded $SO_2{-}H_2O$ complex has also been predicted.[45,54,57,64] However, the chalcogen bonded complex examined here is the one found by microwave experiment[21] and the one that the dissociation reactions discussed here lead to, according to our IRC computations.

B. Vibrational Frequencies

We computed anharmonic frequencies for sulfonic acid and the *cis* and *trans* rotamers of sulfurous acid as described in Section II E. As discussed in Section III A 3, the previously reported third rotamer is of no physical significance, so its anharmonic frequencies were not computed.

1. Comparison to Existing Predicted Spectra

TABLE VIII: The harmonic and anharmonic frequencies of *cis*-suflurous acid computed by reference 24 at MP2/aug-cc-pVTZ and by this work at CCSD(T)-F12b/cc-pVT(T+d)Z-F12. All frequencies are in cm^{-1}.

Mode	Ref. 24 Harmonic	Our Harmonic	Δ Harmonic	Ref. 24 Scaled	Our Anharmonic	Δ Anharmonic
$\nu_1(a')$	3699	3726	+27	3514	3544	+30
$\nu_2(a')$	1255	1266	+11	1192	1248	+56
$\nu_3(a')$	1108	1123	+15	1053	1094	+41
$\nu_4(a')$	780	809	+29	741	792	+51
$\nu_5(a')$	485	504	+19	461	499	+38
$\nu_6(a')$	407	422	+15	387	391	+4
$\nu_7(a')$	340	346	+6	323	330	+7
$\nu_8(a'')$	3697	3724	+27	3512	3543	+31
$\nu_9(a'')$	1082	1096	+14	1028	1077	+49
$\nu_{10}(a'')$	769	806	+37	731	784	+53
$\nu_{11}(a'')$	442	460	+18	420	438	+18
$\nu_{12}(a'')$	126	122	−4	119	83	−36

Voegele *et al.* reported harmonic and scaled harmonic frequencies at the MP2/aug-cc-pVTZ level of theory for *cis*-sulfurous acid.[24] To demonstrate the reliability of our values in the absence of experimental observation, we provide a qualitative explanation of the disagreement. Per Table VIII, the mean unsigned error in their harmonic frequencies compared to ours is 19 cm^{-1}, and the mean unsigned error in anharmonic frequencies is 34 cm^{-1}. We see that both the level of theory from reference 24 and scaling of harmonic frequencies to approximate anharmonic frequencies are large sources of error in predicted frequencies. Modes 1 and 8 are −OH stretches and should not be sensitive to the basis set used to treat sulfur, but −OH stretches are known to be sensitive to anharmonicity. We can thus qualitatively assign that error to the use of MP2 for −OH stretches. Modes 4 and 10 are stretches of the HO−S bonds. As documented in Table I, the basis set is responsible

for the majority of the error in the HO−S bond length at that level of theory, so we assume that much of the harmonic frequency error is due to the lack of tight d functions on sulfur. Hence, the largest updates in frequencies appear for the modes we would suspect to be most sensitive to an improvement in theory.

Further, the updates are significant across the infrared spectrum. Reference 24 tended to *underpredict* harmonic frequencies and *overpredict* frequency lowering due to anharmonicity, leading to an overall red-shifting of the spectrum. Nine of the twelve modes have an overall change of at least 30 cm^{-1}, and three modes have an overall change of more than 50 cm^{-1}. Hence, our predicted vibrational frequencies are a large improvement on previous predictions.

Lastly, we point out that although previous researchers published anharmonic frequencies for select OH stretch modes of hydrated complexes of sulfurous and sulfonic acids,[73] it is not clear which OH stretch a given frequency corresponds to, so no comparison is possible.

2. Spectra and Resonances

We next discuss the resonances present in *cis*-sulfurous acid, *trans*-sulfurous acid, and sulfonic acid. Although the *cis*-sulfurous and *trans*-sulfurous acids have a similar number of resonances, the loss of symmetry between the rotamers means that the two rotamers have different normal modes, and thus have resonances of different complexity.

The fundamental frequencies of *cis*-sulfurous acid are given in Table IX, and the predicted spectra is given in Figure 8. The theoretical treatment of *cis*-sulfurous acid is the most complicated of the three species considered due to its resonance structure. We detected five resonances, which we treated with four increasingly large resonance polyads. The first polyad treats the resonance between ν_6 and the $2\nu_{12}$ as well as the resonance between ν_7 and the $2\nu_{12}$ polyad. We find that the three states are strongly mixed, and the wavefunctions for each of the fundamentals are only about 60% of the corresponding normal mode and 30-40% of the other normal mode. The next polyad starts as a resonance between ν_{11} and the $\nu_6+\nu_{12}$ combination band. It is also necessary to treat the $\nu_7 + 2\nu_{12}$ state and the $3\nu_{12}$ state for a 4-state polyad. We note that this requires deperturbing the resonance denominator for $\nu_{11}, \nu_7, \nu_{12}$, even though there is not a direct Fermi resonance between them. The final computed harmonic frequency changes significantly upon removing any state from the polyad, so all four states are essential for the description of this fundamental.

TABLE IX: The harmonic frequencies, shifts from harmonic to anharmonic frequency, and anharmonic frequencies of *cis*-sulfurous acid computed at CCSD(T)-F12b/cc-pV(T+d)Z-F12, and infrared intensities computed as described in Section II E. All frequencies are in cm^{-1}, and intensities are in km mol^{-1}.

Mode	Description	Harmonic	Shift	Anharmonic	Intensity
$\nu_1(a')$	Symmetric OH stretch	3726	-182	3544	96
$\nu_2(a')$	S=O stretch	1266	-18	1248	153
$\nu_3(a')$	Symmetric SOH bend	1123	-28	1095	14
$\nu_4(a')$	Symmetric S$-$OH stretch	809	-17	792	139
$\nu_5(a')$	SO_3 umbrella	504	-5	499	18
$\nu_6(a')$	O$-$S$-$O scissor	422	-31	391	126
$\nu_7(a')$	*anti*-SO stretch	346	-14	330	2
$\nu_8(a'')$	Antisymmetric OH stretch	3724	-181	3543	40
$\nu_9(a'')$	Antisymmetric SOH bend	1096	-18	1078	60
$\nu_{10}(a'')$	Antisymmetric S$-$OH stretch	806	-22	784	302
$\nu_{11}(a'')$	S=O rocking	460	-22	438	47
$\nu_{12}(a'')$	Antisymmetric SOH wagging	122	-39	83	13

The third polyad arises due to the resonance between ν_{10} and the $\nu_7 + \nu_{11}$ combination band. This can further interact with the aforementioned states, leading a total of 10 states in the polyad. We find that most of the frequency changes come from removal of resonance denominators, bringing the frequency down to 782 cm^{-1}. The interaction with the other states adjusts it slightly to a final 784 cm^{-1}. The final resonance is between ν_2 and the $\nu_{11} + \nu_{10}$ combination band. As both ν_{10} and ν_{11} are present in large polyads, these produce a final polyad consisting of 29 states. The effective Hamiltonian changes the fundamental frequency by < 1 cm^{-1} compared to the simply deperturbed frequency. In this situation, the zeroth-order one- and two-quanta states are nearly degenerate ($\Delta E = 0.07$ cm^{-1}); however, they are coupled by a small matrix element (2.93 cm^{-1}). In the fully-coupled description, weak perturbative interactions with other nearby states raise their energy separation until the interaction strength becomes vanishingly small. Thus the deperturbed frequency is nearly the same as the corresponding frequency from the effective Hamiltonian treatment. Such a situation has been called a pseudoresonance.[114] For this reason, the large polyad is irrelevant to an accurate description of the fundamental; only deperturbation is necessary. As a

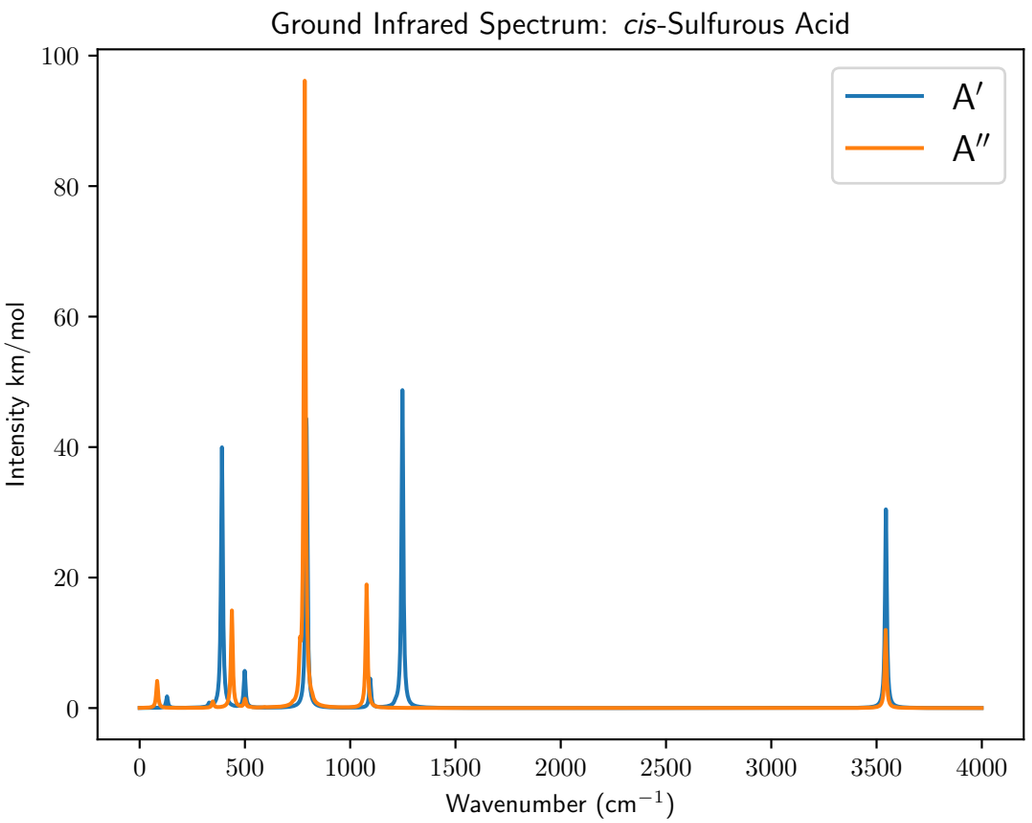

FIG. 8: The *cis*-sulfurous acid theoretical spectrum computed at the CCSD(T)-F12b/cc-pV(T+d)Z-F12 level of theory in this work. Frequencies and descriptions of normal modes are given in Table IX. Stick spectra are generated by Lorentzian curves with full width half max of 2 cm^{-1} and integrated area equal to the total intensity.

result of all these resonance interactions, the following combination bands and overtones borrow at least 1 km mol^{-1} of intensity: $2\nu_{12}$ at 130 cm^{-1}, $\nu_6 + \nu_{12}$ at 347 cm^{-1}, $\nu_7 + \nu_{12}$ at 500 cm^{-1}, $\nu_7 + \nu_{11}$ at 761 cm^{-1}, $\nu_6 + \nu_{11}$ at 818 cm^{-1}, $\nu_{10} + \nu_{11}$ at 1215 cm^{-1}.

The spectrum of *trans*-sulfurous acid, with fundamentals reported in Table X and spectrum shown in Figure 9, is less involved and has four resonances. Interaction between the ν_9 and the $2\nu_{12}$ states leads to a large resonance denominator. After removing it, variational treatment changes the ν_9 fundamental by a moderate 6 cm^{-1}. The ν_6 fundamental band and the $\nu_8 + \nu_{11}$ combination band have a large resonance denominator, but interact weakly. The variational treatment changes the frequencies by < 1 cm^{-1} from the deperturbed frequencies. The other resonance is between ν_7 and the $\nu_9 + \nu_{11}$ combination band, which can further interact with the $\nu_{11} + 2\nu_{12}$ state. Predictions

of the ν_7 band require primarily deperturbation treatment. The frequency changes by only 1 cm^{-1} due to interaction with the $\nu_9 + \nu_{11}$ and is unchanged when $\nu_{11} + 2\nu_{12}$ is added to the polyad. Finally, ν_5 can interact with the $\nu_6 + \nu_{11}$ combination band, which can in turn interact with $\nu_8 + 2\nu_{11}$. Yet again, although the resonance constant must be deperturbed, the fundamental of ν_5 is insensitive to effective Hamiltonian treatmnent, changing by 2 cm^{-1} in the two-state polyad, but not changing further when the polyad is extended to 3 states. Hence, the choice of states to include in the effective Hamiltonian is not a significant source of uncertainty for any of these resonances. However, the polyads give rise to combination bands with appreciable intensity: $2\nu_{12}$ at 479 cm^{-1}, $\nu_9 + \nu_{11}$ at 679 cm^{-1}, $\nu_8 + \nu_{11}$ at 759 cm^{-1}, and $\nu_6 + \nu_{11}$ at 1041 cm^{-1}.

TABLE X: The harmonic frequencies, shifts from harmonic to anharmonic frequency, and anharmonic frequencies of *trans*-sulfurous acid computed at CCSD(T)-F12b/cc-pV(T+d)Z-F12, and infrared intensities computed as described in Section II E. All frequencies are in cm^{-1}, and intensities are in km mol^{-1}.

Mode	Description	Harmonic	Shift	Anharmonic	Intensity
ν_1	*anti*-OH stretch	3782	−179	3603	79
ν_2	*syn*-OH stretch	3716	−184	3532	70
ν_3	S=O stretch	1291	−18	1273	144
ν_4	out of phase SOH bend	1127	−26	1101	57
ν_5	in phase SOH bend	1111	−25	1086	92
ν_6	*syn*-SO stretch	806	−17	789	179
ν_7	*anti*-SO stretch	774	−19	755	214
ν_8	SO_3 umbrella	512	−7	505	34
ν_9	*syn*-OS=O scissoring	477	−36	441	45
ν_{10}	*anti*-OS=O scissoring	412	−21	391	21
ν_{11}	OH torsion	294	−38	256	64
ν_{12}	O−S−O scissor	237	−6	231	49

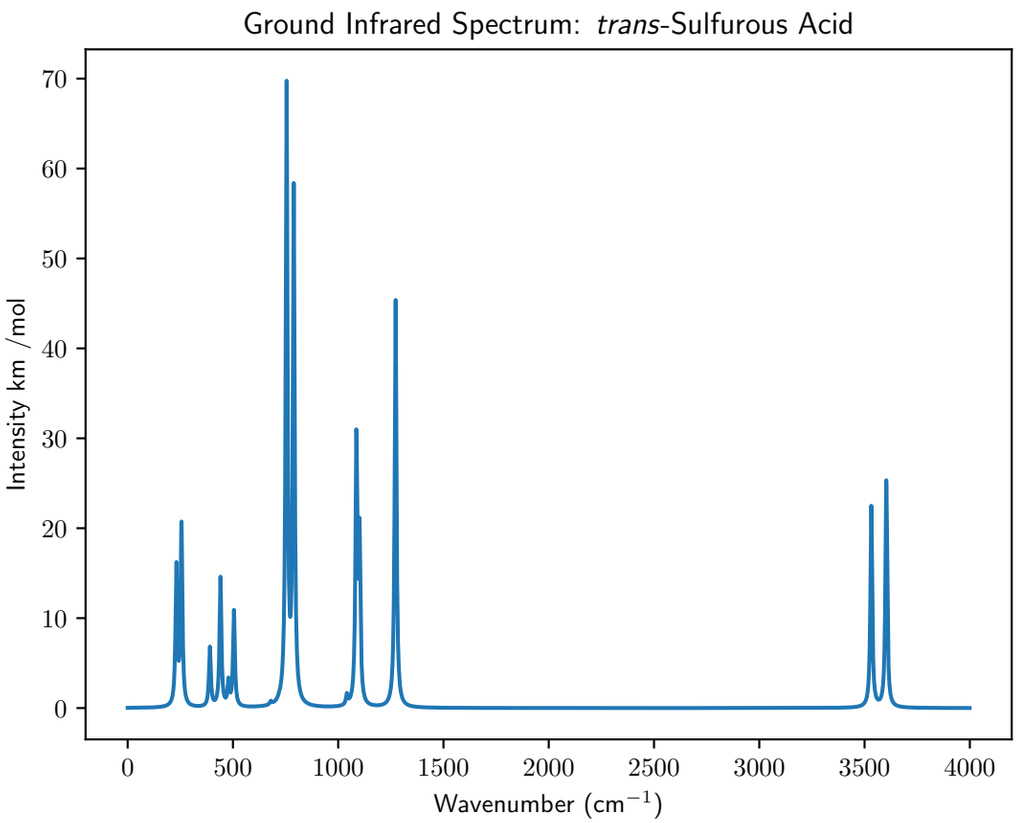

FIG. 9: The *trans*-sulfurous acid theoretical spectrum computed at the CCSD(T)-F12b/cc-pV(T+d)Z-F12 level of theory in this work. Frequencies and descriptions of normal modes are given in Table X. Stick spectra are generated by Lorentzian curves with full width half max of 2 cm^{-1} and integrated area equal to the total intensity.

TABLE XI: The harmonic frequencies, shifts from harmonic to anharmonic frequency, and anharmonic frequencies of sulfonic acid computed at CCSD(T)-F12b/cc-pV(T+d)Z-F12, and infrared intensities computed as described in Section II E. All frequencies are in cm^{-1}, and intensities are in km mol^{-1}.

Mode	Description	Harmonic	Shift	Anharmonic	Intensity
ν_1	OH stretch	3790	−186	3603	121
ν_2	SH stretch	2662	−124	2538	35
ν_3	Antisymmetric SO stretch	1471	−28	1443	248
ν_4	Symmetric SO stretch	1234	−20	1214	175
ν_5	HOS bend, hydride bend to *syn*, out of phase	1186	−30	1156	11
ν_6	HOS bend, hydride bend to OH, in phase	1133	−29	1104	34
ν_7	HOS bend, hydride bend to *syn*, in phase	1097	−27	1070	7
ν_8	S−OH stretch	878	−21	857	185
ν_9	SO_3H umbrella	599	−11	588	54
ν_{10}	OSO scissor	481	−6	475	29
ν_{11}	*syn*-OSOH scissor	445	−19	426	25
ν_{12}	S−OH twist	303	−27	276	81

Theoretically, the vibrational spectrum of sulfonic acid is exceptionally simple. There is a single resonance between the $\nu_5 + \nu_3$ combination band and ν_2. This gives intensity to a weak band at 2599 cm^{-1}. Intense bands should be observable at $3603, 1443, 1214,$ and 857 cm^{-1}. The predicted fundamental frequencies are in Table XI, with the spectrum in Figure 10.

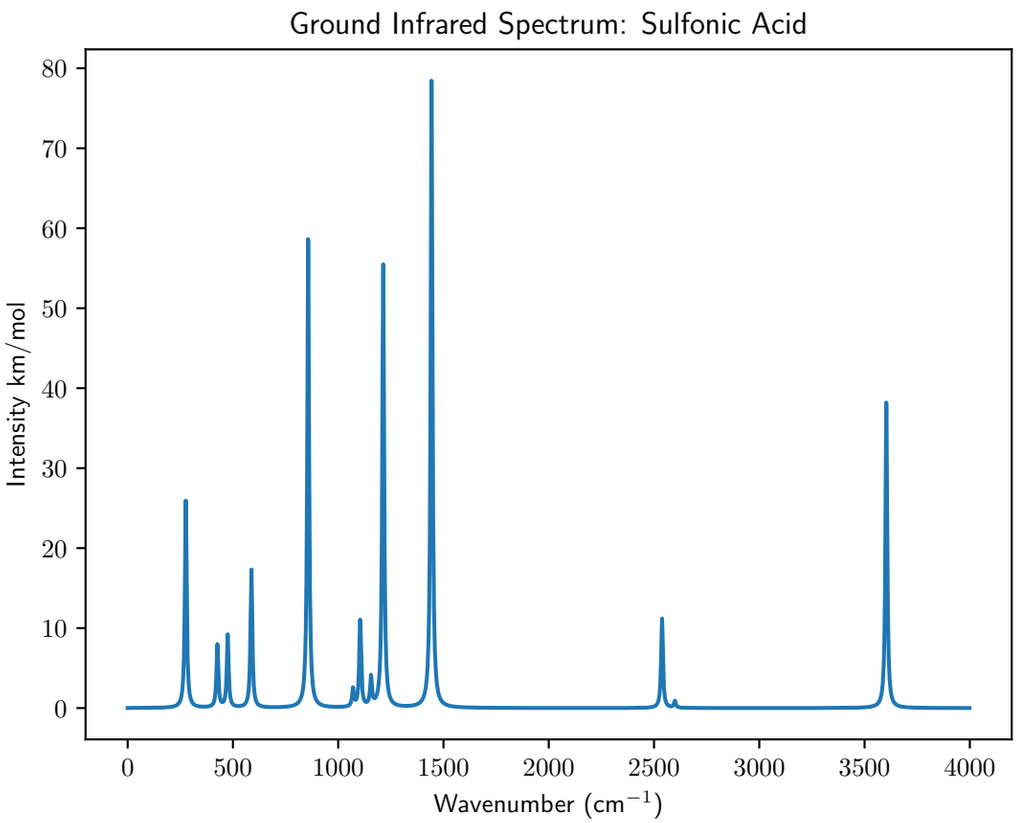

FIG. 10: The sulfonic acid theoretical spectrum computed at the CCSD(T)-F12b/cc-pV(T+d)Z-F12 level of theory in this work. Frequencies and descriptions of normal modes are given in Table XI. Stick spectra are generated by Lorentzian curves with full width half max of 2 cm^{-1} and integrated area equal to the total intensity.

3. *Distinguishability of Spectra*

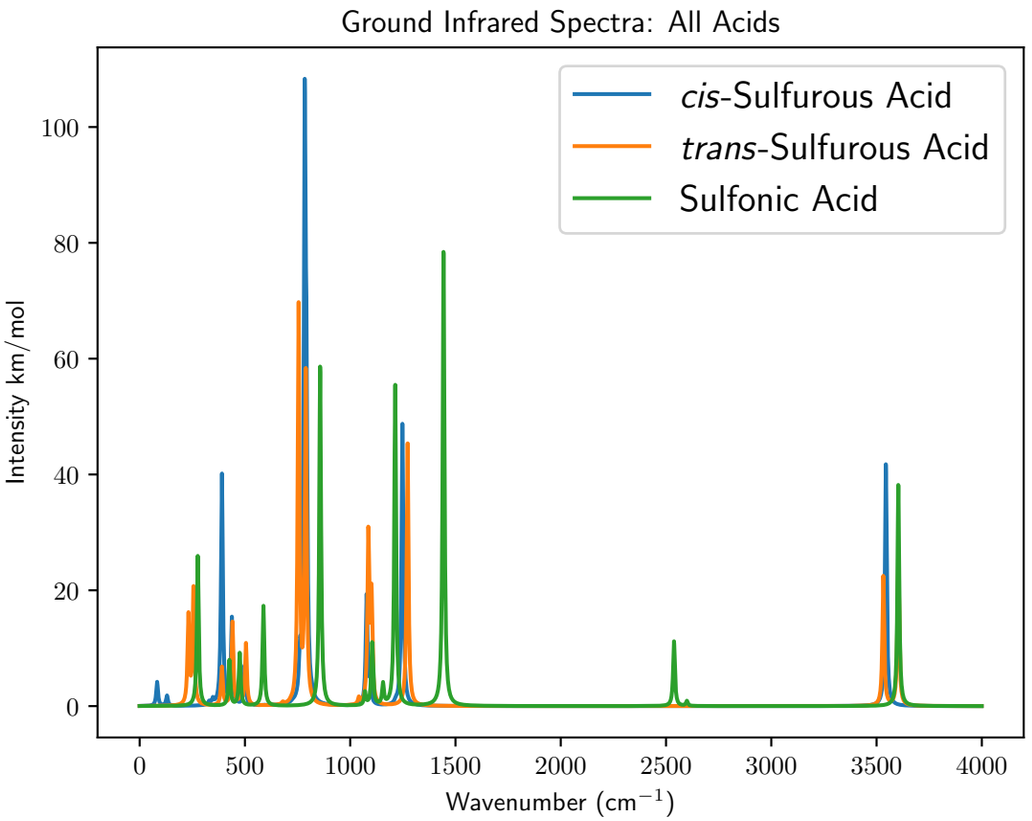

FIG. 11: An overlay of the three spectra of Figures 8, 9, 10. Stick spectra are generated by Lorentzian curves with full width half max of 2 cm^{-1} and integrated area equal to the total intensity.

To discuss the possibility of differentiating the three species in a sample, the three spectra are overlaid in Figure 11. Unsurprisingly, the *cis* and *trans* spectra, being rotamers of the same molecule, are difficult to separate. The task is made more difficult by the possibility of sulfonic acid. However, given the large energy barrier (Figure 2) necessary to form sulfonic acid from either the separated SO_2 and H_2O reactants (Section III A 5) or a sulfurous acid rotamer (Section III A 4), sulfonic acid may very well not be present in an experimental sample. The presence of sulfonic acid can be confirmed or denied by looking for the large band at 1443 cm^{-1}. If no band in that region of the spectrum is present, then sulfonic acid can be removed from consideration. This would greatly simplify the remaining spectral analysis. The *cis*-spectrum has its two OH stretch

peaks at 3543 and 3544 cm^{-1}, but the *trans*-spectrum has them at 3532 and 3603. Sulfonic acid has its own OH stretch peak at 3603, but if sulfonic acid is not present, the existence of *trans*-sulfurous acid can be probed by looking for the peak at 3603 cm^{-1}.

A more robust way to identify a mixture of the three is by the S=O stretch peaks. All three spectra have intense peaks in the 1200-1300 cm^{-1} region that are well separated from any other peaks of the three species. The *cis*-sulfurous acid peak is at 1248 cm^{-1}, the *trans*-sulfurous acid peak is at 1273 cm^{-1}, and the sulfonic acid peak is at 1214 cm^{-1}. It may be surprising that the S=O stretching frequency should be sensitive to the rotation of a OH group. We presume that much of this effect is due to the contracting of the S=O bond from 1.451 to 1.439 between the *cis* and *trans* rotamers, respectively, documented in Tables I and II. We believe this change in bond length is due to the hyperconjugation described in detail at the end of Section III A 1.

IV. CONCLUSIONS

We have studied the singlet $SO_2 + H_2O$ potential energy surface, including the long sought but elusive sulfurous and sulfonic acids. The results of this research have yielded the most accurate structures, energetics, and fundamental vibrational frequencies to date. During this process, we resolved contradictions and solved open questions in the literature. Most notably:

1. The *cis* rotamer of sulfurous acid lies below the *trans* rotamer by 1.1 kcal mol^{-1} ΔH_{0K}, and the rotational barrier to convert from *cis* to *trans* is 1.6 kcal mol^{-1}, which is lower than previously predicted.[1] Further, that the *cis* rotamer is lower in ΔH_{0K} is not due to intramolecular hydrogen bonding, as previously thought,[32] but due to hyperconjugation of oxygen lone pair orbitals with the SO bonding orbitals.

2. Although the third sulfurous acid rotamer reported by Li, Bu, and coworkers[32] is a minimum on the electronic potential energy surface, it is of no physical significance. The barriers for the third rotamer to rotate to one of the other rotamers is smaller than the differences in zero-point vibrational energies.

3. The approximately 40 kcal mol^{-1} discrepancies between the two reports of the isomerization barrier between sulfurous acid and sulfonic acid[65,70] are due to the fact that the reporters

found different transition states, one leading to *cis*-sulfurous acid and the other leading to *trans*-sulfurous acid.

4. The complex of SO_2 and H_2O lies 8.5 kcal mol^{-1} below the *cis* rotamer in ΔH_{0K}. Previous reports indicating the energy difference was on the order of 1 kcal mol^{-1} were computed with density functionals inappropriate for this system.

5. Accurate computations on the sulfurous and sulfonic acid systems require a large basis set on sulfur. Inadequate basis sets can lead to 8 kcal mol^{-1} errors in energies, errors of more than 0.04 Å in bond lengths, and errors on the order of 20 cm^{-1} in harmonic frequencies. In particular, for correlation consistent basis sets, tight d functions are essential.

6. The infrared vibrational spectra of *cis*-sulfurous acid, *trans*-sulfurous acid, and sulfonic acid can all be distinguished from each other by consideration of the S=O stretching peaks at 1248, 1273, and 1214 cm^{-1}, respectively. These peaks are separated by at least 25 cm^{-1} from any other intense peak from the three species.

V. SUPPLEMENTARY MATERIAL

See supplementary material for geometries and detailed information about convergence criteria for all stationary points, all focal point tables, an extended analysis of energy sensitivity to electronic structure, trajectories for all IRC calculations, discussion of the misidentification of a triplet sulfurous acid transition state of previous work, and detailed information about the anharmonic vibrational calculations.

VI. ACKNOWLEDGMENTS

We acknowledge helpful discussions with Gregory Pullen about the spectroscopic interpretation of our own results and the existing experiments, Dr. Marcus Bartlett and Dr. Wesley D. Allen about the use of the INTDER program, Dr. Preston R. Hoobler about natural bonding analyses, and Dr. Huidong Li for bringing the functional sensitivity of the sulfurous acid dissociation energy to our attention. We acknowledge discussions with Professor D. J. Donaldson, Professor Henrik G. Kjaergaard, Professor Joseph Francisco, and Professor Josep Anglada regarding reports of

sulfurous acid on the triplet potential surface. We acknowledge support from the U.S. Department of Energy, Office of Basic Energy Sciences, Chemical Sciences Division, Computational and Theoretical (CTC) Program, Grant DE-SC0018412. This research used resources of the National Energy Research Scientific Computing Center (NERSC), a U.S. Department of Energy Office of Science User Facility at Berkeley operated under Contract No. DE-AC02-05CH11231. Figures of molecular structures were created with the CYLView program.[115]

REFERENCES

[1]A. F. Voegele, C. S. Tautermann, T. Loerting, A. Hallbrucker, E. Mayer, and K. R. Liedl, Chem. Eur. J. **8**, 5644 (2002).

[2]D. Sülzle, M. Verhoeven, J. K. Terlouw, and H. Schwarz, Angew. Chem. Int. Ed. **27**, 1533 (1988).

[3]R. K. Sinha, D. Scuderi, P. Maitre, B. Chiavarino, M. E. Crestoni, and S. Fornarini, J. Phys. Chem. Lett. **6**, 1605 (2015).

[4]M. Falk and P. A. Giguère, Can. J. Chem. **36**, 1121 (1958).

[5]L. H. Jones and E. McLaren, J. Chem. Phys. **28**, 995 (1958).

[6]A. R. Davis and R. M. Chatterjee, J. Solution Chem. **4**, 399 (1975).

[7]Z. Zhang and G. E. Ewing, Spectrochim. Acta A **58**, 2105 (2002).

[8]E. D. Risberg, L. Eriksson, J. Mink, L. G. M. Pettersson, M. Y. Skripkin, and M. Sandström, Inorg. Chem. **46**, 8332 (2007).

[9]Y. Beyad, R. Burns, G. Puxty, and M. Maeder, Dalton Trans. **43**, 2147 (2014).

[10]J. P. Guthrie, Can. J. Chem. **57**, 454 (1979).

[11]R. Goldberg and V. Parker, J. Res. Natl. Bur. Stand. **90**, 341 (1985).

[12]C. E. Vanderzee and L. A. Noll, J. Chem. Thermodyn. **19**, 417 (1987).

[13]F. J. Millero, J. B. Hershey, G. Johnson, and J.-Z. Zhang, J. Atmos. Chem. **8**, 377 (1989).

[14]F. P. Terraglio and R. M. Manganelli, J. Air Pollut. Control Assoc. **17**, 403 (1967).

[15]L. Nord, J. Mol. Spec. **96**, 27 (1983).

[16]T. L. Tso and E. K. C. Lee, J. Phys. Chem. **88**, 2776 (1984).

[17]A. Schriver, L. Schriver, and J. Perchard, J. Mol. Spec. **127**, 125 (1988).

[18]S. Hirabayashi, F. Ito, and K. M. T. Yamada, J. Chem. Phys. **125**, 034508 (2006).

[19]T. L. Tarbuck and G. L. Richmond, J. Am. Chem. Soc. **127**, 16806 (2005).

[20]T. L. Tarbuck and G. L. Richmond, J. Am. Chem. Soc. **128**, 3256 (2006).

[21]K. Matsumura, F. J. Lovas, and R. D. Suenram, J. Chem. Phys. **91**, 5887 (1989).

[22]K. L. Knappenberger and A. W. Castleman, J. Chem. Phys. **122**, 154306 (2005).

[23]T. E. Dermota, D. P. Hydutsky, N. J. Bianco, and A. W. Castleman, J. Phys. Chem. A **109**, 8254 (2005).

[24]A. F. Voegele, T. Loerting, C. S. Tautermann, A. Hallbrucker, E. Mayer, and K. R. Liedl, Icarus **169**, 242 (2004).

[25]M. Garozzo, D. Fulvio, O. Gomis, M. Palumbo, and G. Strazzulla, Planet. Space Sci. **56**, 1300 (2008).

[26]R. W. Carlson, J. S. Kargel, S. Douté, L. A. Soderblom, and J. B. Dalton, in *Springer Praxis Books* (Springer Berlin Heidelberg, 2007) pp. 193–229.

[27]M. Moore, R. Hudson, and R. Carlson, Icarus **189**, 409 (2007).

[28]Z. Kaňuchová, P. Boduch, A. Domaracka, M. E. Palumbo, H. Rothard, and G. Strazzulla, Astron. Astrophys. **604**, A68 (2017).

[29]T. M. Townsend, A. Allanic, C. Noonan, and J. R. Sodeau, J. Phys. Chem. A **116**, 4035 (2012).

[30]D. J. Donaldson, J. A. Kroll, and V. Vaida, Sci. Rep. **6** (2016), 10.1038/srep30000.

[31]T. Loerting, K. R. Liedl, and R. T. Kroemer, Chem. Comm. , 999 (2000).

[32]P. Li, Z.-Y. Ma, W.-H. Wang, Z.-T. Shen, S.-W. Bi, H.-T. Sun, and Y.-X. Bu, ChemPhysChem **11**, 696 (2009).

[33]J. Liu, S. Fang, W. Liu, M. Wang, F.-M. Tao, and J. yao Liu, J. Phys. Chem. A **119**, 102 (2014).

[34]J. Liu, S. Fang, Z. Wang, W. Yi, F.-M. Tao, and J. yao Liu, Environ. Sci. Technol. **49**, 13112 (2015).

[35]J. Liu, S. Fang, Q. Bing, F.-M. Tao, and J. yao Liu, Comput. Theor. Chem. **1076**, 11 (2016).

[36]F. Sheng, L. Jingjing, C. Yu, T. Fu-Ming, D. Xuemei, and L. Jing-yao, RSC Adv. **8**, 7988 (2018).

[37]G. Lv, A. B. Nadykto, X. Sun, C. Zhang, and Y. Xu, Chemosphere **205**, 275 (2018).

[38]J. Bang, M. A. Shoaib, C. H. Choi, and H. Kang, ACS Earth Space Chem. **1**, 503 (2017).

[39]J. A. Kroll, B. N. Frandsen, H. G. Kjaergaard, and V. Vaida, J. Phys. Chem. A **122**, 4465 (2018).

[40]J. M. Anglada, M. T. C. Martins-Costa, J. S. Francisco, and M. F. Ruiz-López, Phys. Chem. Chem. Phys. **21**, 9779 (2019).

[41]J. S. Francisco and J. M. Anglada, (private communication).

[42]N. C. Baird and K. F. Taylor, J. Comp. Chem. **2**, 225 (1981).

[43]P. M. Holland and A. Castleman, J. Photochem. **16**, 347 (1981).

[44]R. R. Squires, Int. J. Mass. Spectrom. Ion Phys. **117**, 565 (1992).

[45]P. L. M. Plummer, J. Mol. Struct. **307**, 119 (1994).

[46]R. E. Brown and F. Barber, J. Phys. Chem. **99**, 8071 (1995).

[47]W.-K. Li and M. L. McKee, J. Phys. Chem. A **101**, 9778 (1997).

[48]E. Bishenden and D. J. Donaldson, J. Phys. Chem. A **102**, 4638 (1998).

[49]A. H. Otto and R. Steudel, European Journal of Inorganic Chemistry **2000**, 617 (2000).

[50]T. Loerting and K. R. Liedl, J. Phys. Chem. A **105**, 5137 (2001).

[51]J. R. T. Johnson and I. Panas, J. Phys. Chem. A **106**, 184 (2002).

[52]L. Wang and J. Zhang, J. Mol. Spec. **581**, 129 (2002).

[53]A. L. Garden, J. R. Lane, and H. G. Kjaergaard, J. Chem. Phys. **125**, 144317 (2006).

[54]J. Cukras and J. Sadlej, J. Mol. Spec. **819**, 41 (2007).

[55]T. A. Ford, J. Mol. Spec. **924-926**, 466 (2009).

[56]R. Steudel and Y. Steudel, Eur. J. Inorg. Chem. **2009**, 1393 (2009).

[57]H. Yang, N. J. Wright, A. M. Gagnon, R. B. Gerber, and B. J. Finlayson-Pitts, Phys. Chem. Chem. Phys. **4**, 1832 (2002).

[58]M. Baer, C. J. Mundy, T.-M. Chang, F.-M. Tao, and L. X. Dang, J. Phys. Chem. B **114**, 7245 (2010).

[59]S. T. Moin, L. H. V. Lim, T. S. Hofer, B. R. Randolf, and B. M. Rode, Inorg. Chem. **50**, 3379 (2011).

[60]S. T. Ota and G. L. Richmond, J. Am. Chem. Soc. **133**, 7497 (2011).

[61]H. Tachikawa, J. Phys. Chem. A **115**, 9091 (2011).

[62]V.-A. Glezakou, B. P. McGrail, and H. T. Schaef, Geochim. Cosmochim. Acta **92**, 265 (2012).

[63]E. S. Shamay, N. A. Valley, F. G. Moore, and G. L. Richmond, Phys. Chem. Chem. Phys. **15**, 6893 (2013).

[64]J. Zhong, C. Zhu, L. Li, G. L. Richmond, J. S. Francisco, and X. C. Zeng, J. Am. Chem. Soc. **139**, 17168 (2017).

[65]A. F. Voegele, C. S. Tautermann, C. Rauch, T. Loerting, and K. R. Liedl, J. Phys. Chem. A **108**, 3859 (2004).

[66]J. M. Younker, T. Saito, M. A. Hunt, A. K. Naskar, and A. Beste, J. Am. Chem. Soc. **135**, 6130 (2013).

[67]S. Shostak, K. Kim, Y. Horbatenko, and C. H. Choi, J. Phys. Chem. A **123**, 8385 (2019).

[68]Y. Tian, Z.-M. Tian, W.-M. Wei, T.-J. He, D.-M. Chen, and F.-C. Liu, Chem. Phys. **335**, 133 (2007).

[69]T. F. Kahan, D. Ardura, and D. J. Donaldson, J. Phys. Chem. A **114**, 2164 (2010).

[70]S. H. Mousavipour, M. Mortazavi, and O. Hematti, J. Phys. Chem. A **117**, 6744 (2013).

[71]T. H. Dunning, K. A. Peterson, and A. K. Wilson, J. Chem. Phys. **114**, 9244 (2001).

[72]A. K. Wilson and T. H. Dunning, J. Phys. Chem. A **108**, 3129 (2004).

[73]M. Kołaski, A. A. Zakharenko, S. Karthikeyan, and K. S. Kim, J. Chem. Theory Comput. **7**, 3447 (2011).

[74]R. D. Bell and A. K. Wilson, Chem. Phys. Lett. **394**, 105 (2004).

[75]A. K. Wilson and T. H. Dunning, J. Chem. Phys. **119**, 11712 (2003).

[76]T. B. Adler, G. Knizia, and H.-J. Werner, J. Chem. Phys. **127**, 221106 (2007).

[77]H.-J. Werner, G. Knizia, and F. R. Manby, Mol. Phys. **109**, 407 (2011).

[78]K. A. Peterson, T. B. Adler, and H.-J. Werner, J. Chem. Phys. **128**, 084102 (2008).

[79]H.-J. Werner, P. J. Knowles, G. Knizia, F. R. Manby, M. Schütz, P. Celani, W. Györffy, D. Kats, T. Korona, R. Lindh, A. Mitrushenkov, G. Rauhut, K. R. Shamasundar, T. B. Adler, R. D. Amos, S. J. Bennie, A. Bernhardsson, A. Berning, D. L. Cooper, M. J. O. Deegan, A. J. Dobbyn, F. Eckert, E. Goll, C. Hampel, A. Hesselmann, G. Hetzer, T. Hrenar, G. Jansen, C. Köppl, S. J. R. Lee, Y. Liu, A. W. Lloyd, Q. Ma, R. A. Mata, A. J. May, S. J. McNicholas, W. Meyer, T. F. Miller III, M. E. Mura, A. Nicklass, D. P. O'Neill, P. Palmieri, D. Peng, K. Pflüger, R. Pitzer, M. Reiher, T. Shiozaki, H. Stoll, A. J. Stone, R. Tarroni, T. Thorsteinsson, M. Wang, and M. Welborn, "Molpro, version 2019.1, a package of ab initio programs," (2019).

[80]R. M. Parrish, L. A. Burns, D. G. A. Smith, A. C. Simmonett, A. E. DePrince, E. G. Hohenstein, U. Bozkaya, A. Y. Sokolov, R. D. Remigio, R. M. Richard, J. F. Gonthier, A. M. James, H. R. McAlexander, A. Kumar, M. Saitow, X. Wang, B. P. Pritchard, P. Verma, H. F. Schaefer, K. Patkowski, R. A. King, E. F. Valeev, F. A. Evangelista, J. M. Turney, T. D. Crawford, and C. D. Sherrill, J. Chem. Theory Comput. **13**, 3185 (2017).

[81]C. Gonzalez and H. B. Schlegel, J. Phys. Chem. **94**, 5523 (1990).

[82]U. Bozkaya, The Journal of Chemical Physics **141**, 124108 (2014).

[83]M. S. Schuurman, S. R. Muir, W. D. Allen, and H. F. Schaefer, J. Chem. Phys. **120**, 11586 (2004).

[84]J. M. Gonzales, C. Pak, R. S. Cox, W. D. Allen, H. F. Schaefer, A. G. Császár, and G. Tarczay, Chem. Eur. J. **9**, 2173 (2003).

[85]A. G. Császár, W. D. Allen, and H. F. Schaefer, J. Chem. Phys. **108**, 9751 (1998).

[86]A. L. L. East and W. D. Allen, J. Chem. Phys. **99**, 4638 (1993).

[87]T. H. Dunning, J. Chem. Phys. **90**, 1007 (1989).

[88]D. E. Woon and T. H. Dunning, J. Chem. Phys. **98**, 1358 (1993).

[89]D. E. Woon and T. H. Dunning, The Journal of Chemical Physics **103**, 4572 (1995).

[90]D. Feller, K. A. Peterson, and T. D. Crawford, J. Chem. Phys. **124**, 054107 (2006).

[91]T. Helgaker, W. Klopper, H. Koch, and J. Noga, J. Chem. Phys. **106**, 9639 (1997).

[92]J. F. Stanton, J. Gauss, L. Cheng, M. E. Harding, D. A. Matthews, and P. G. Szalay, "CFOUR, Coupled-Cluster techniques for Computational Chemistry, a quantum-chemical program package," With contributions from A.A. Auer, R.J. Bartlett, U. Benedikt, C. Berger, D.E. Bernholdt, Y.J. Bomble, O. Christiansen, F. Engel, R. Faber, M. Heckert, O. Heun, M. Hilgenberg, C. Huber, T.-C. Jagau, D. Jonsson, J. Jusélius, T. Kirsch, K. Klein, W.J. Lauderdale, F. Lipparini, T. Metzroth, L.A. Mück, D.P. O'Neill, D.R. Price, E. Prochnow, C. Puzzarini, K. Ruud, F. Schiffmann, W. Schwalbach, C. Simmons, S. Stopkowicz, A. Tajti, J. Vázquez, F. Wang, J.D. Watts and the integral packages MOLECULE (J. Almlöf and P.R. Taylor), PROPS (P.R. Taylor), ABACUS (T. Helgaker, H.J. Aa. Jensen, P. Jørgensen, and J. Olsen), and ECP routines by A. V. Mitin and C. van Wüllen. For the current version, see http://www.cfour.de.

[93]K. A. Peterson and T. H. Dunning, J. Chem. Phys. **117**, 10548 (2002).

[94]W. Klopper, J. Comp. Chem. **18**, 20 (1997).

[95]G. Tarczay, A. G. Császár, W. Klopper, and H. M. Quiney, Mol. Phys. **99**, 1769 (2001).

[96]N. C. Handy, Y. Yamaguchi, and H. F. Schaefer, J. Chem. Phys. **84**, 4481 (1986).

[97]H. Sellers and P. Pulay, Chem. Phys. Lett. **103**, 463 (1984).

[98]P. J. Knowles and H.-J. Werner, Chem. Phys. Lett. **145**, 514 (1988).

[99]H.-J. Werner and P. J. Knowles, J. Chem. Phys. **89**, 5803 (1988).

[100]Intder2005 is a general program developed by Wesley D. Allen and co-workers which performs various vibrational analyses and higher-order nonlinear transformations among force field representations.

[101]W. D. Allen and A. G. Császár, J. Chem. Phys. **98**, 2983 (1993).

[102]W. D. Allen, A. G. Császár, V. Szalay, and I. M. Mills, Mol. Phys. **89**, 1213 (1996).

[103]H. H. Nielsen, Rev. Mod. Phys. **23**, 90 (1951).

[104]D. Clabo, W. D. Allen, R. B. Remington, Y. Yamaguchi, and H. F. Schaefer, Chem. Phys. **123**, 187 (1988).

[105]A. M. Rosnik and W. F. Polik, Mol. Phys. **112**, 261 (2013).

[106]J. M. L. Martin, T. J. Lee, P. R. Taylor, and J.-P. François, J. Chem. Phys. **103**, 2589 (1995).

[107]X. Chen, C. Tao, L. Zhong, Y. Gao, W. Yao, and S. Li, Chem. Phys. Lett. **608**, 272 (2014).

[108]T. Stefan and R. Janoschek, J. Mol. Modeling **6**, 282 (2000).

[109]E. Tiemann, J. Phys. Chem. Ref. Data **3**, 259 (1974).

[110]S. Saito, J. Mol. Spec. **30**, 1 (1969).

[111]J. K. Watson, J. Mol. Spec. **48**, 479 (1973).

[112]E. D. Glendening, C. R. Landis, and F. Weinhold, J. Comp. Chem. **34**, 1429 (2013).

[113]A. C. Legon, Phys. Chem. Chem. Phys. **19**, 14884 (2017).

[114]H. Schneider, K. M. Vogelhuber, F. Schinle, J. F. Stanton, and J. M. Weber, The Journal of Physical Chemistry A **112**, 7498 (2008).

[115]CYLview, 1.0b; Legault, C. Y., Université de Sherbrooke, 2009 (http://www.cylview.org).

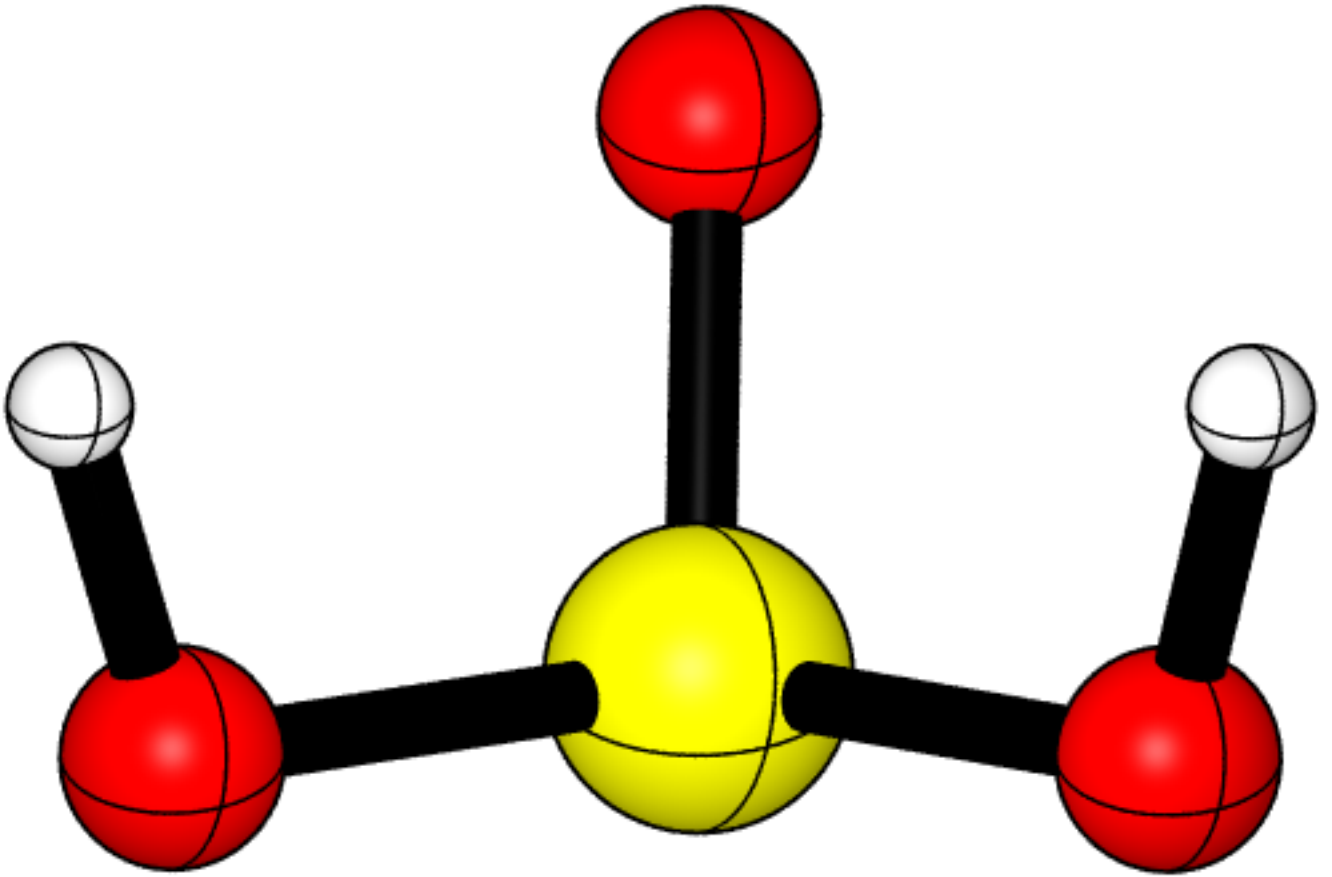

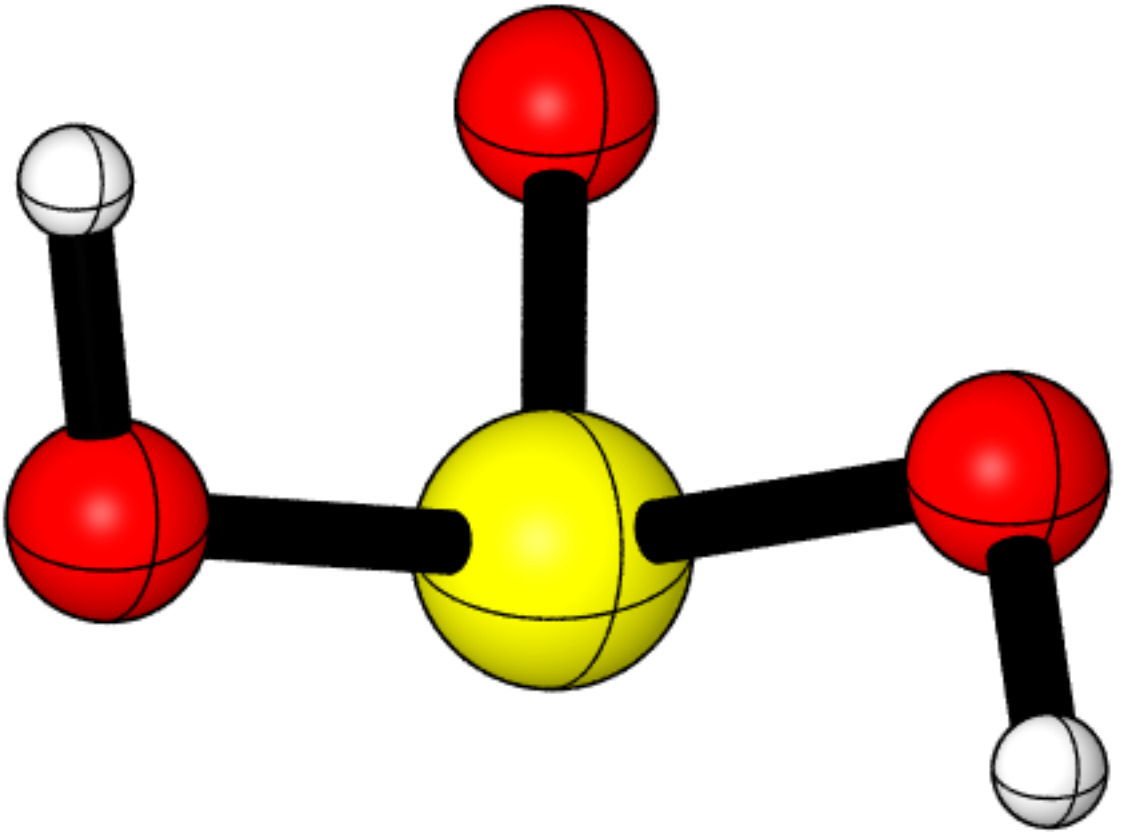

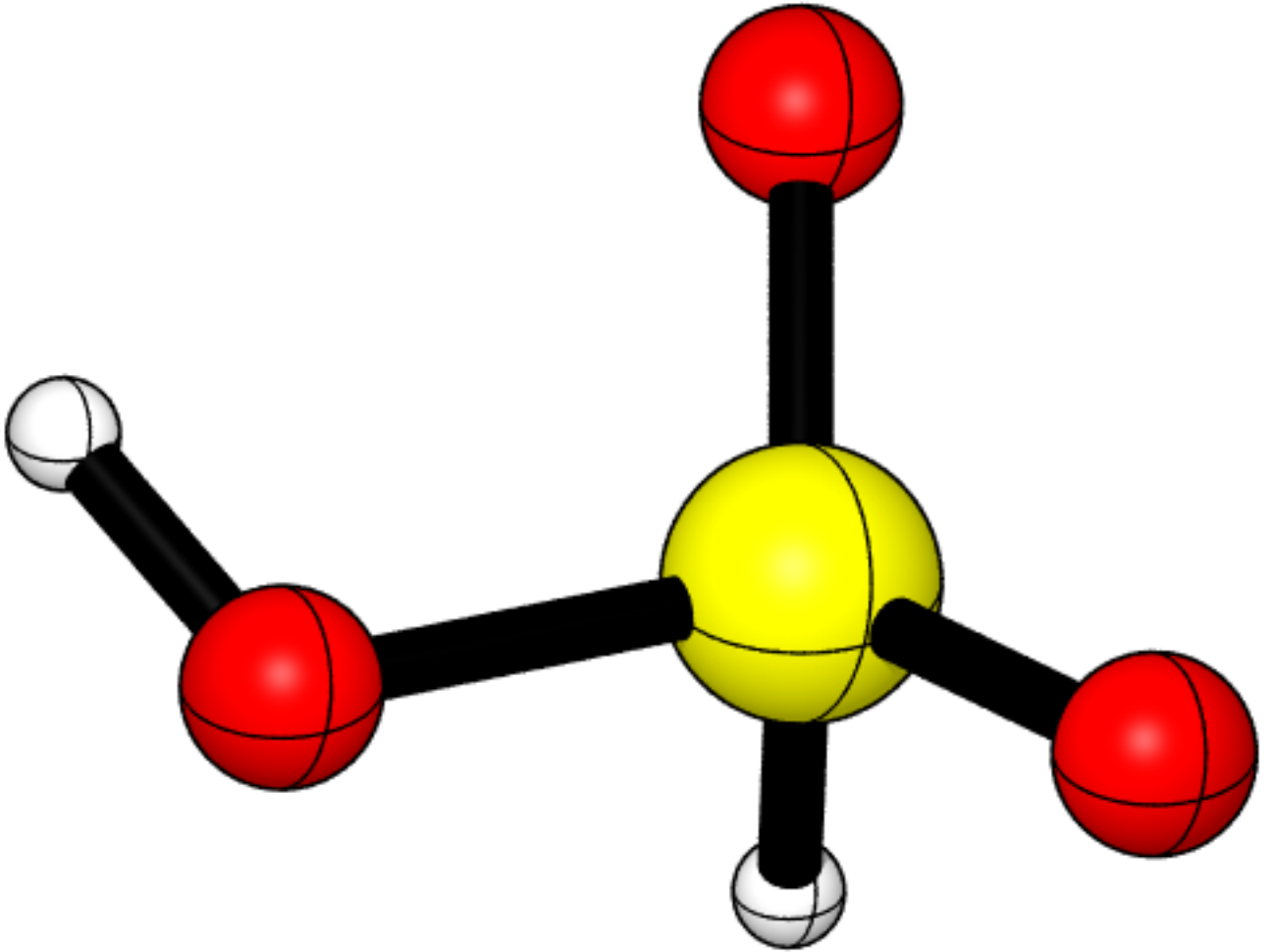

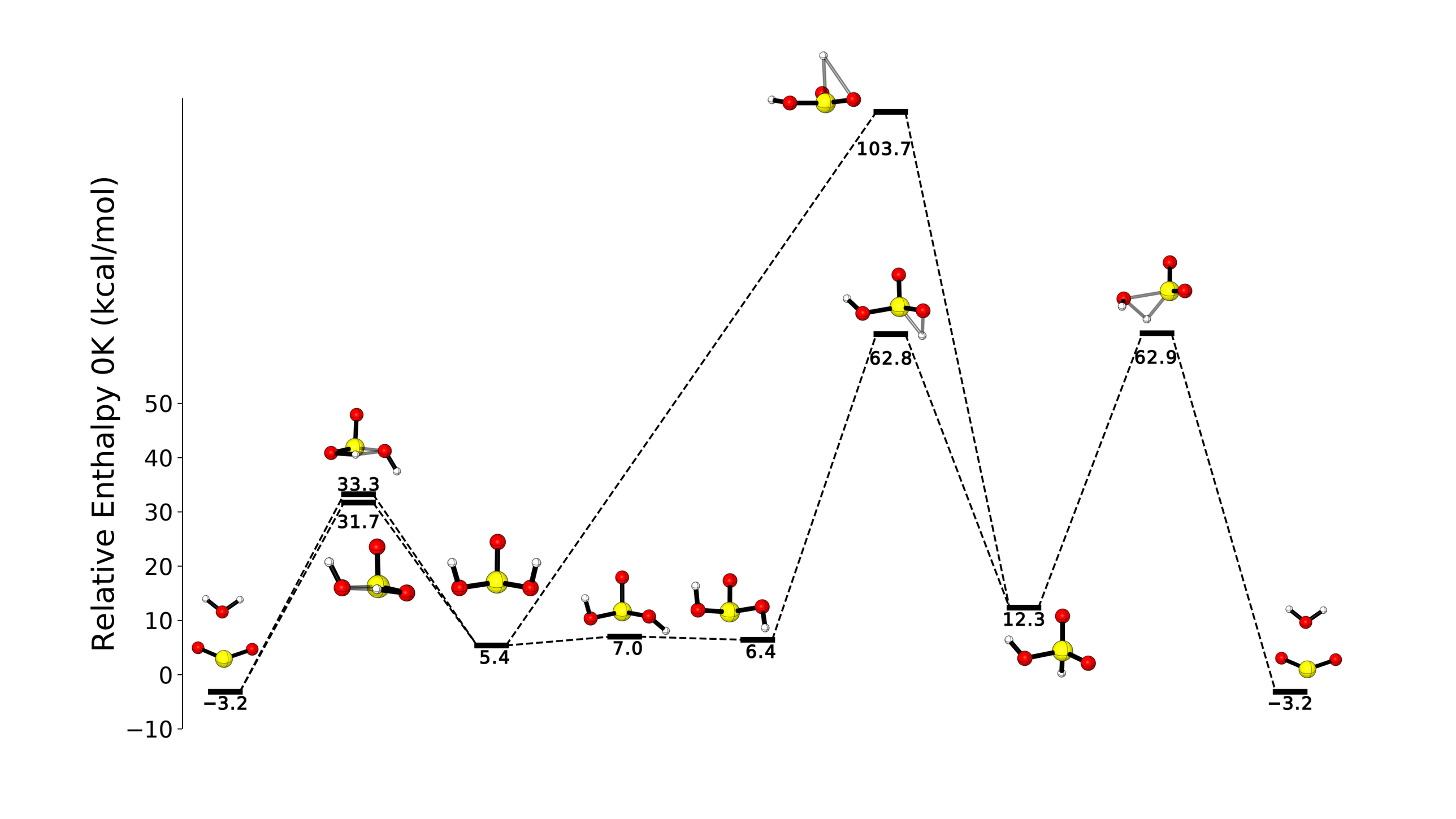
Relative Enthalpy 0K (kcal/mol)
50
40
30
20
10
0
−10
−3.2
33.3
31.7
5.4
7.0
6.4
103.7
62.8
12.3
62.9
−3.2

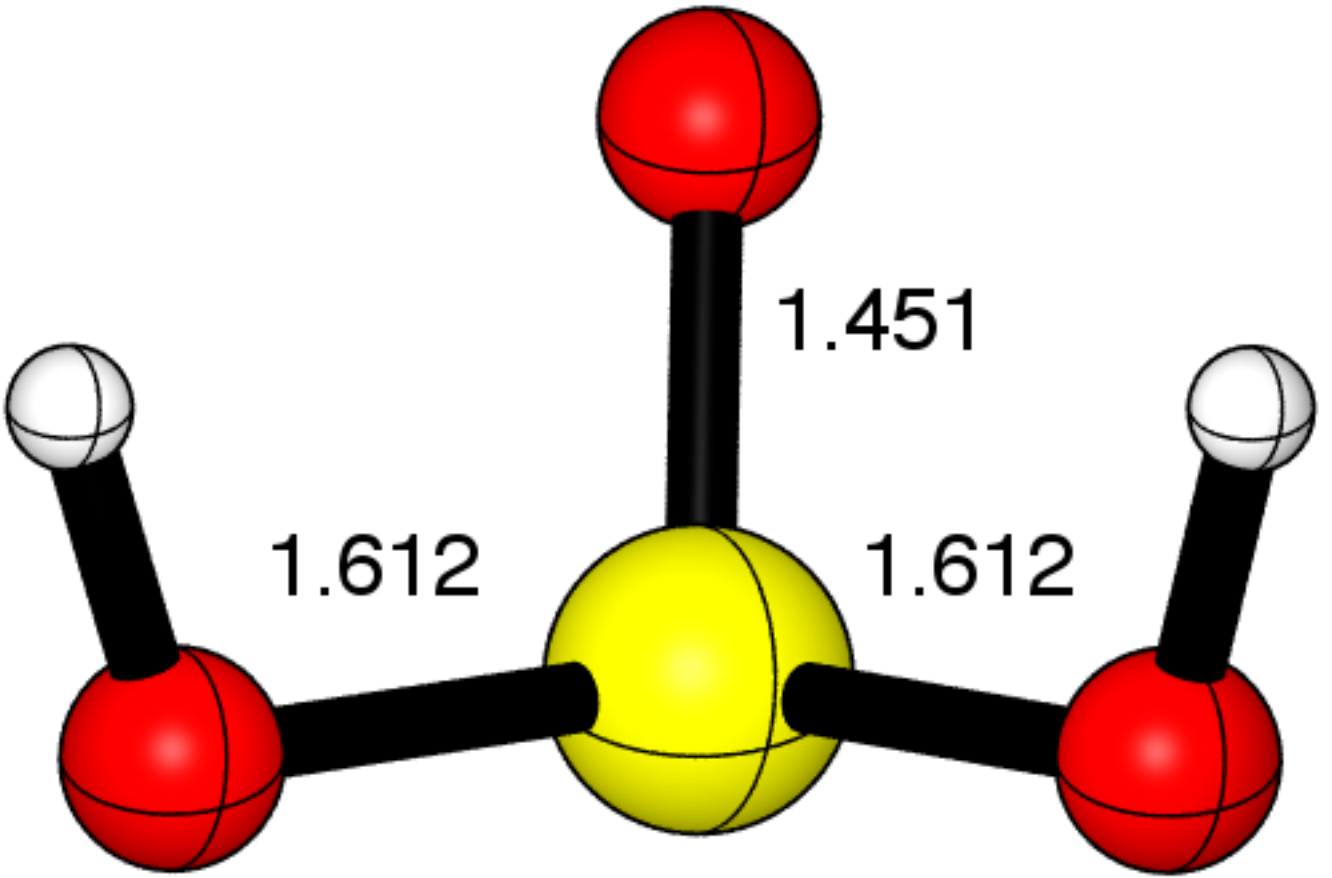
1.451
1.612
1.612

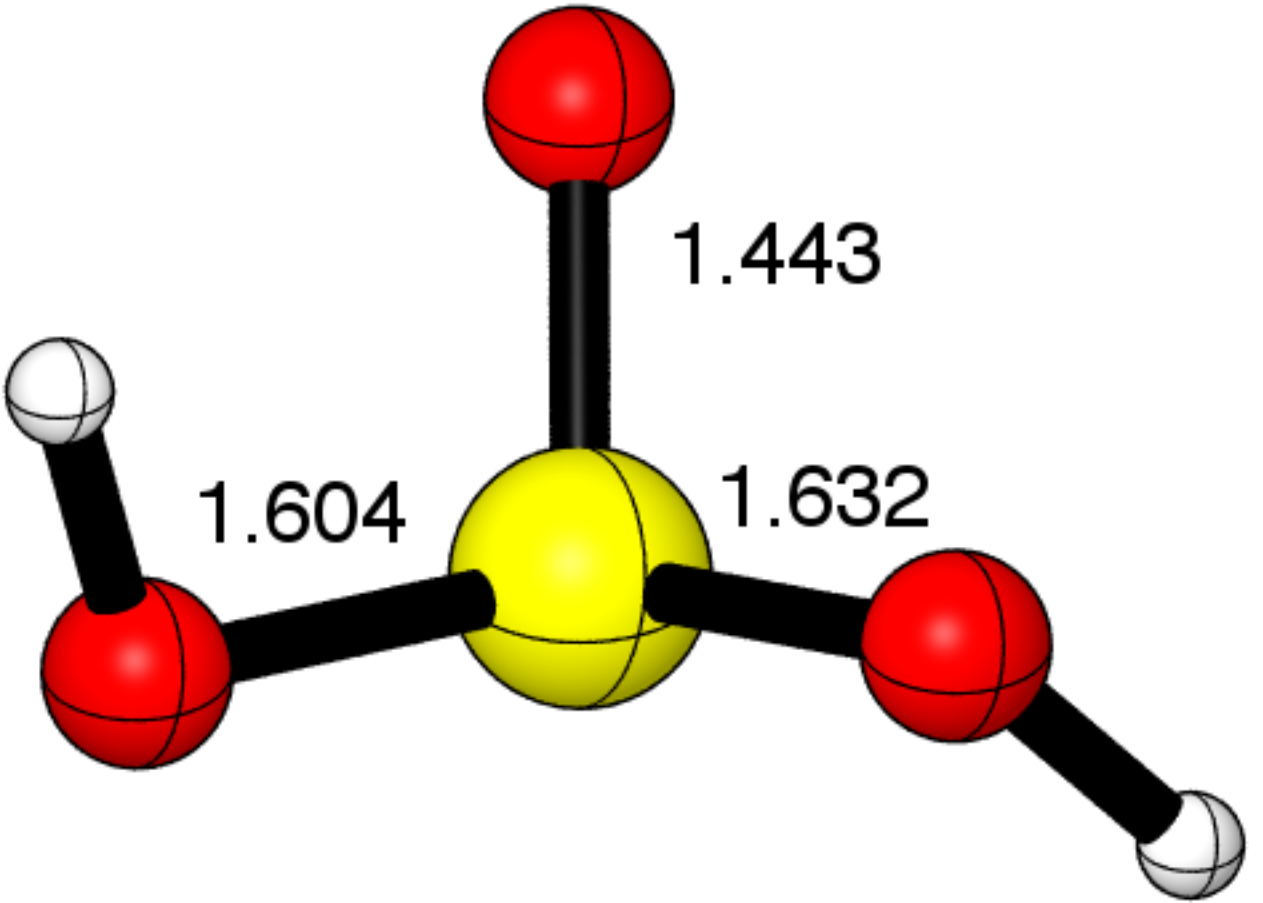
1.443
1.604
1.632

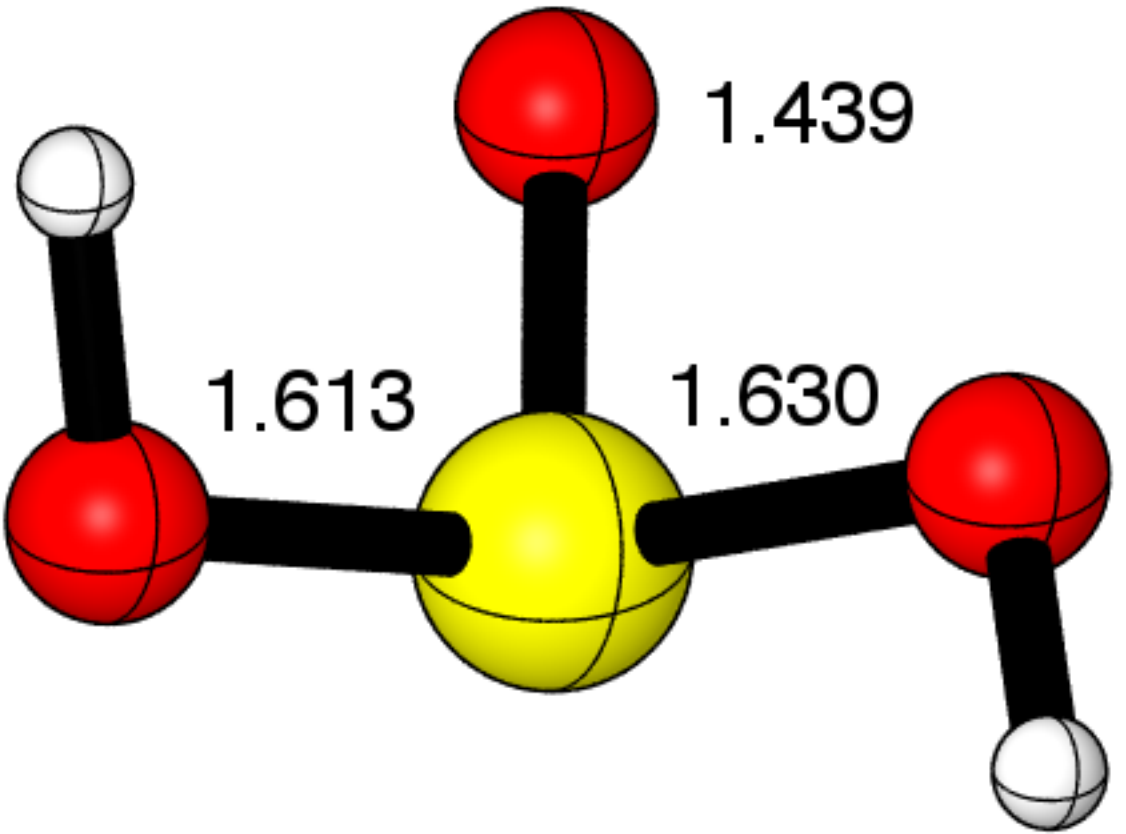
1.439
1.613
1.630

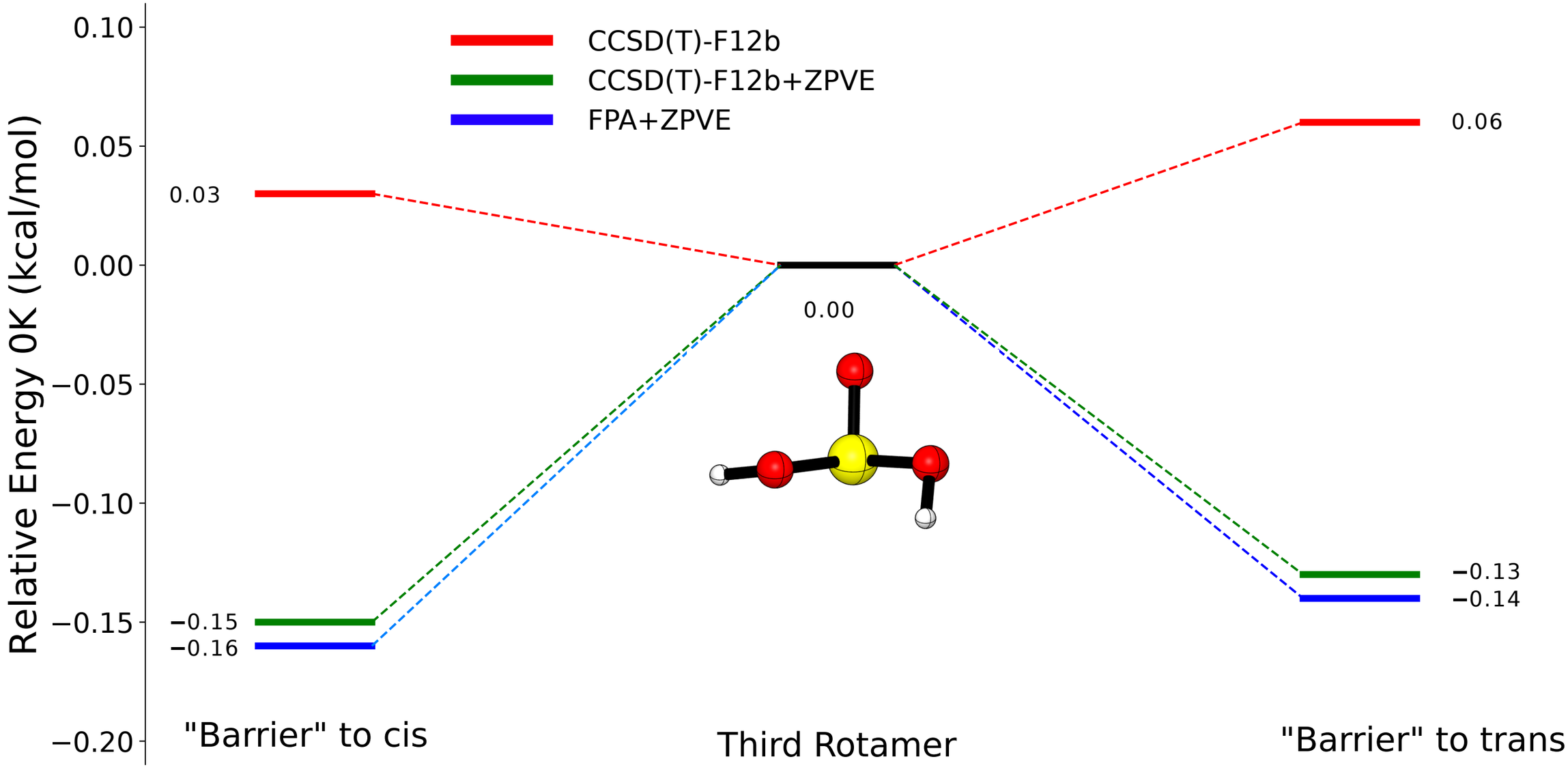
CCSD(T)-F12b
CCSD(T)-F12b+ZPVE
FPA+ZPVE
Relative Energy 0K (kcal/mol)
0.10
0.05
0.00
−0.05
−0.10
−0.15
−0.20
0.03
0.00
0.06
−0.15
−0.16
−0.13
−0.14
"Barrier" to cis
Third Rotamer
"Barrier" to trans

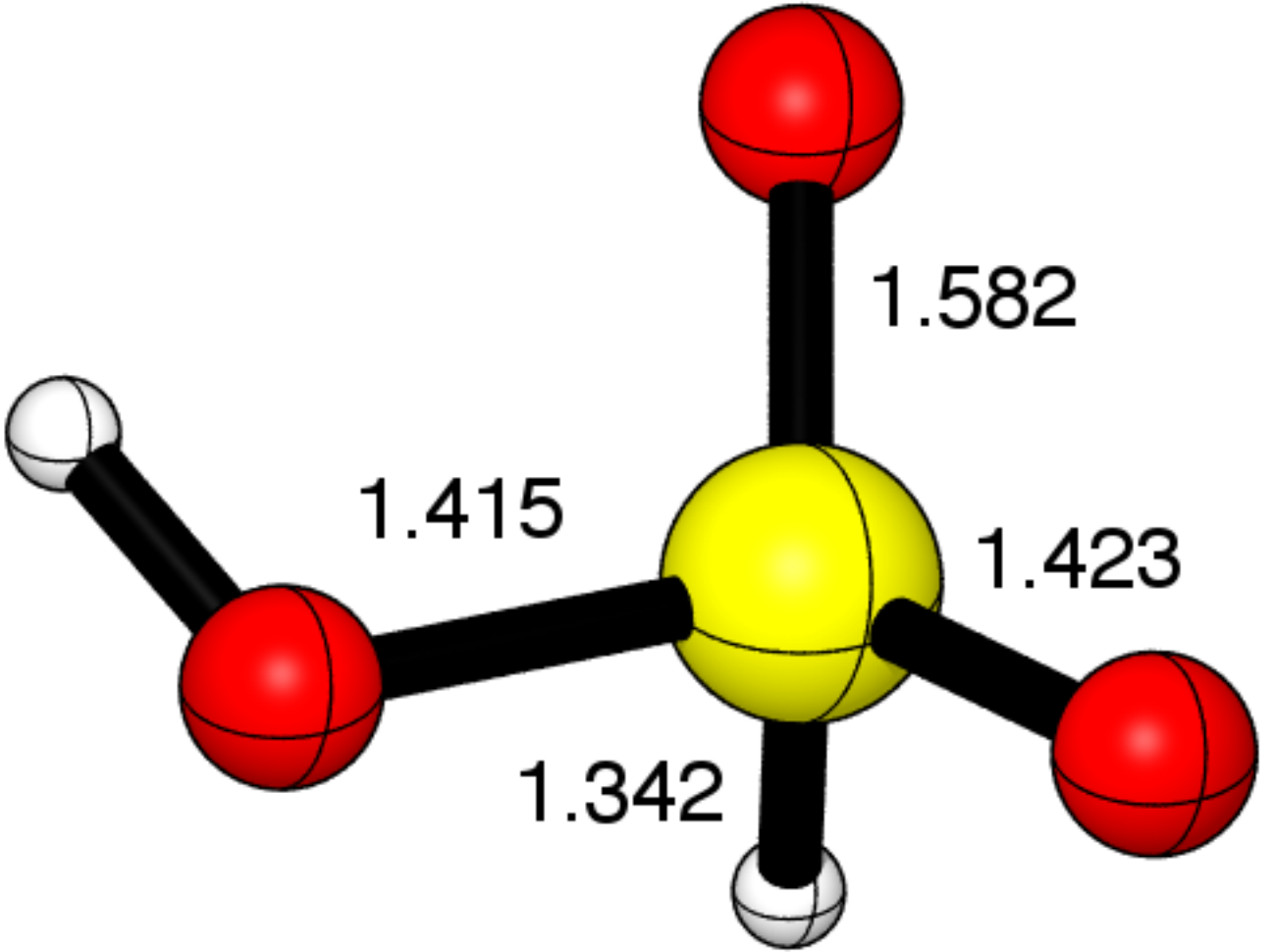
1.582
1.415
1.423
1.342

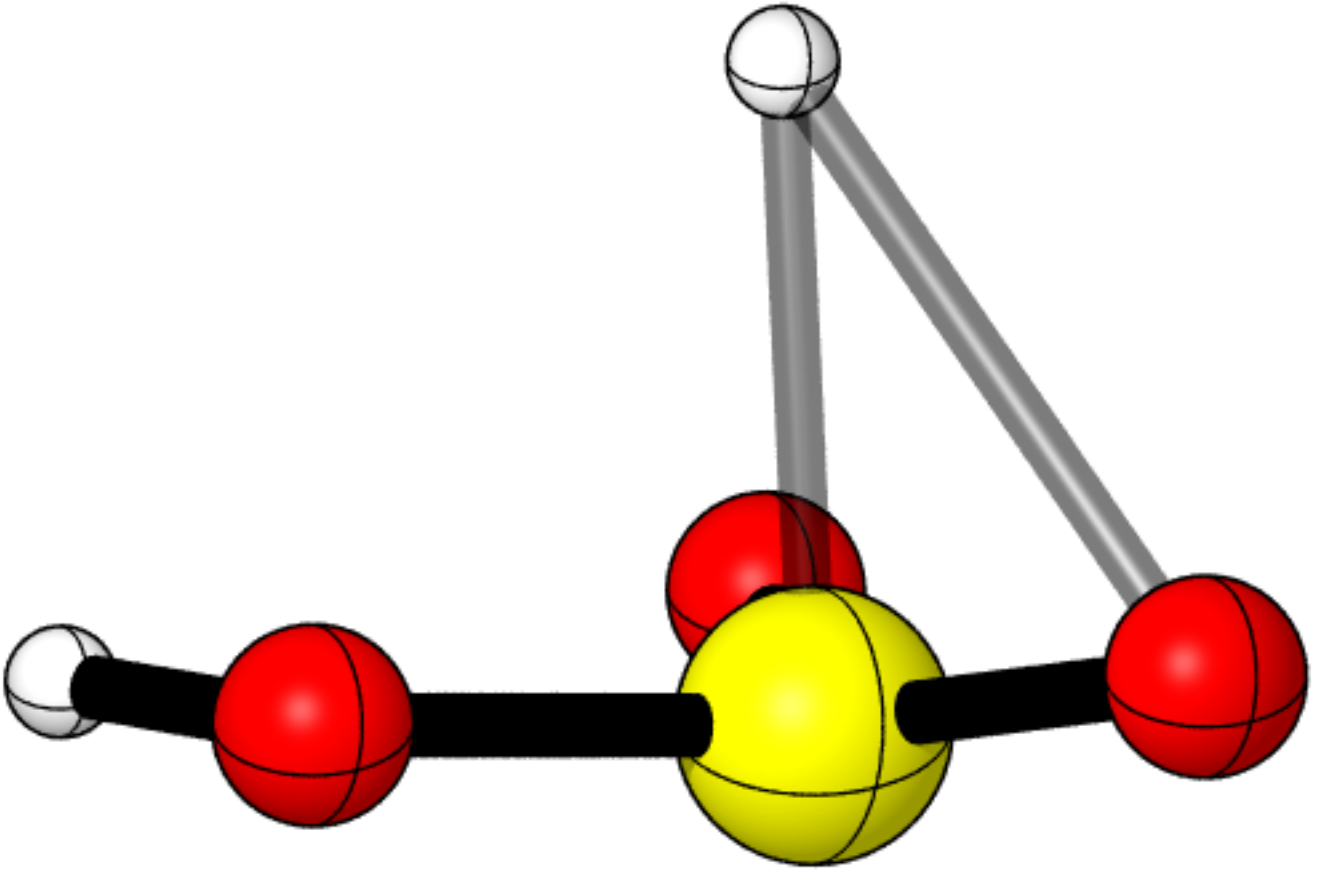

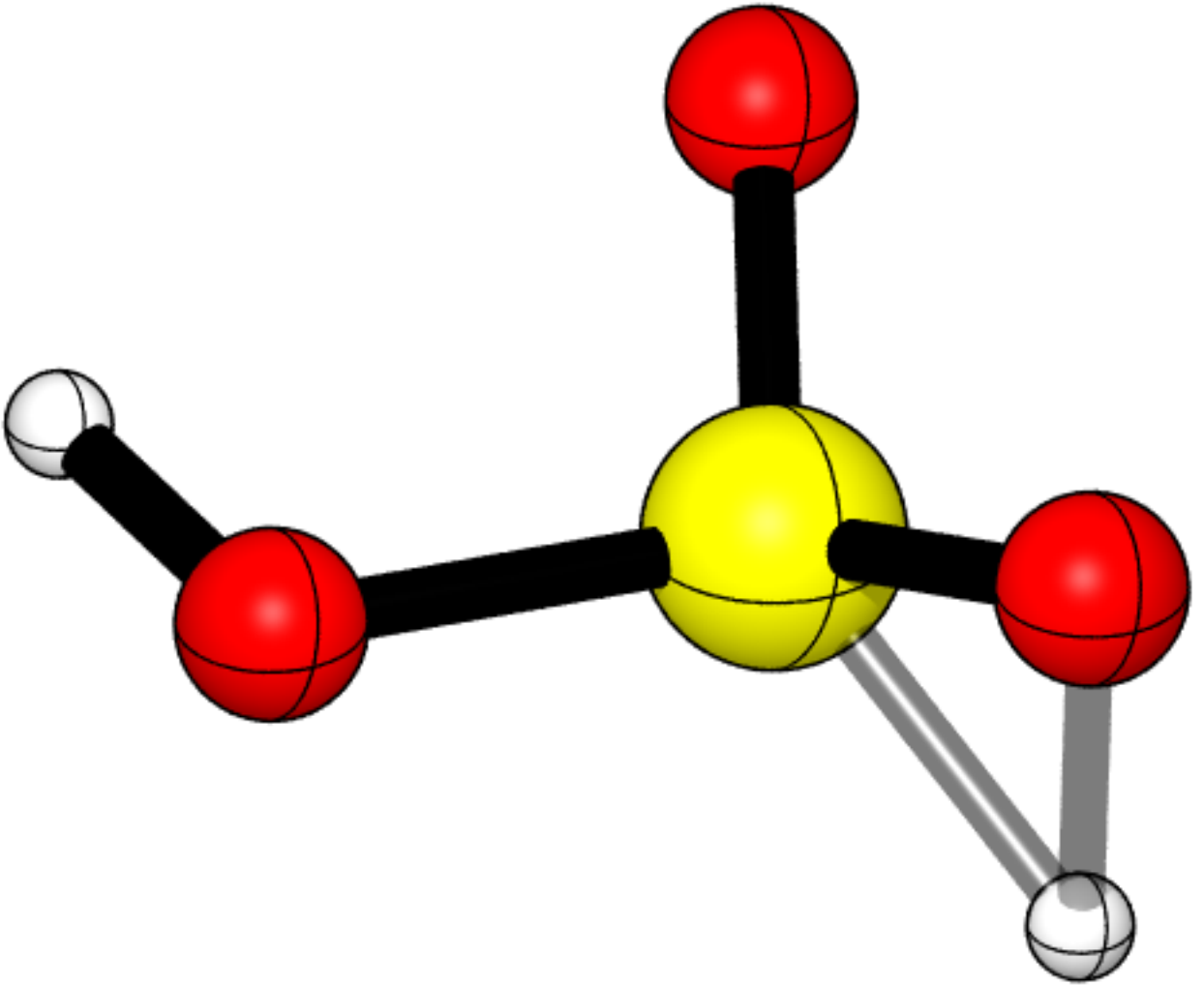

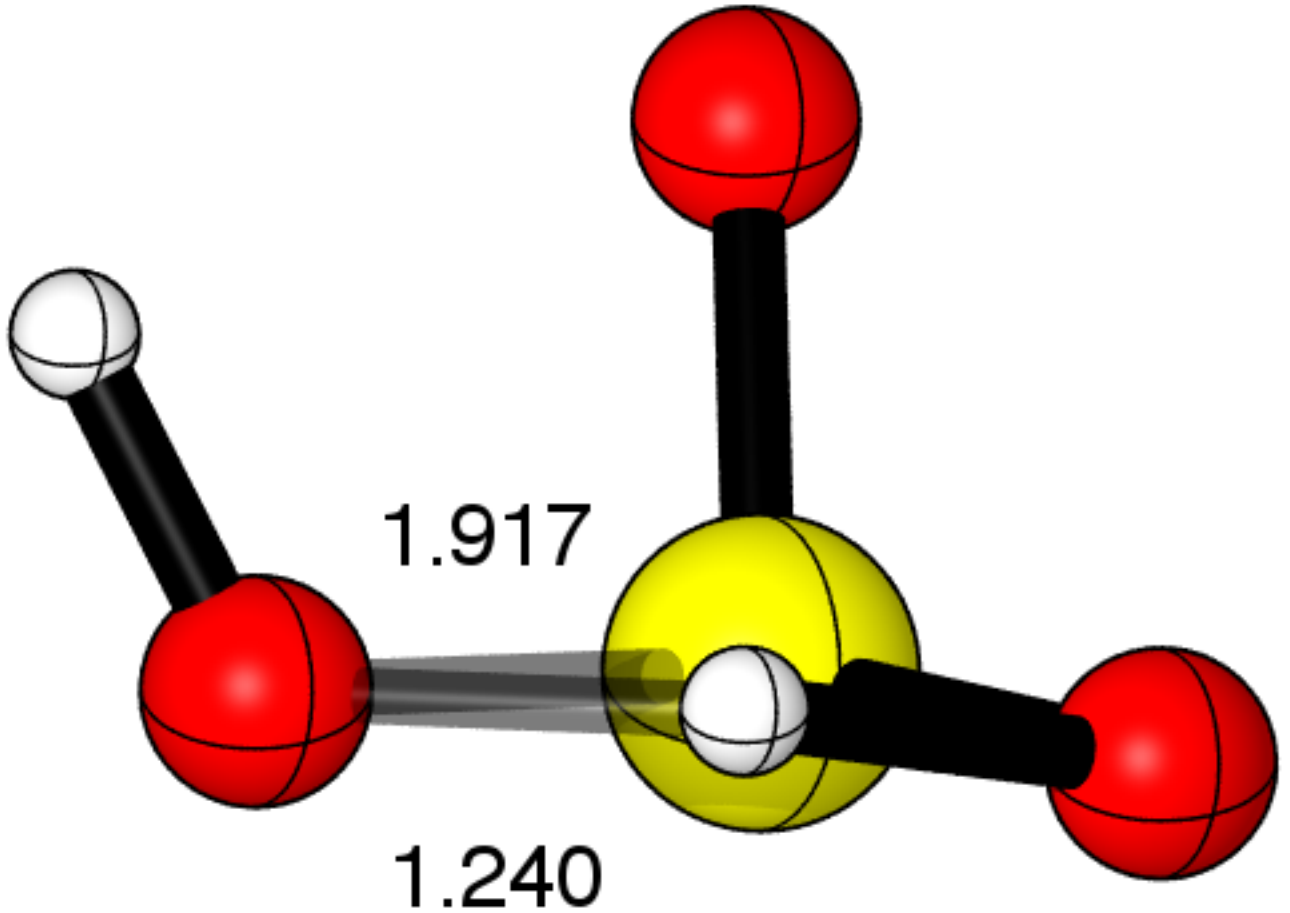
1.917
1.240

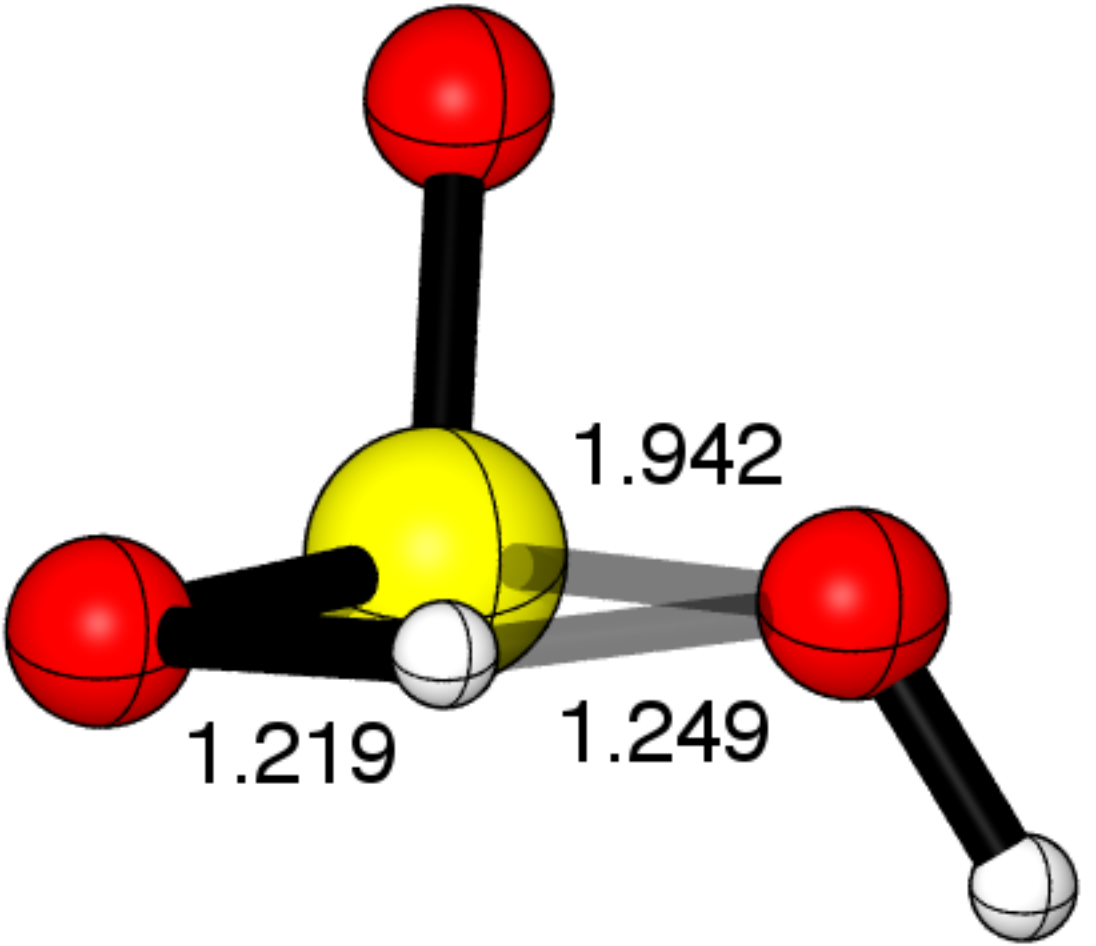
1.942
1.219
1.249

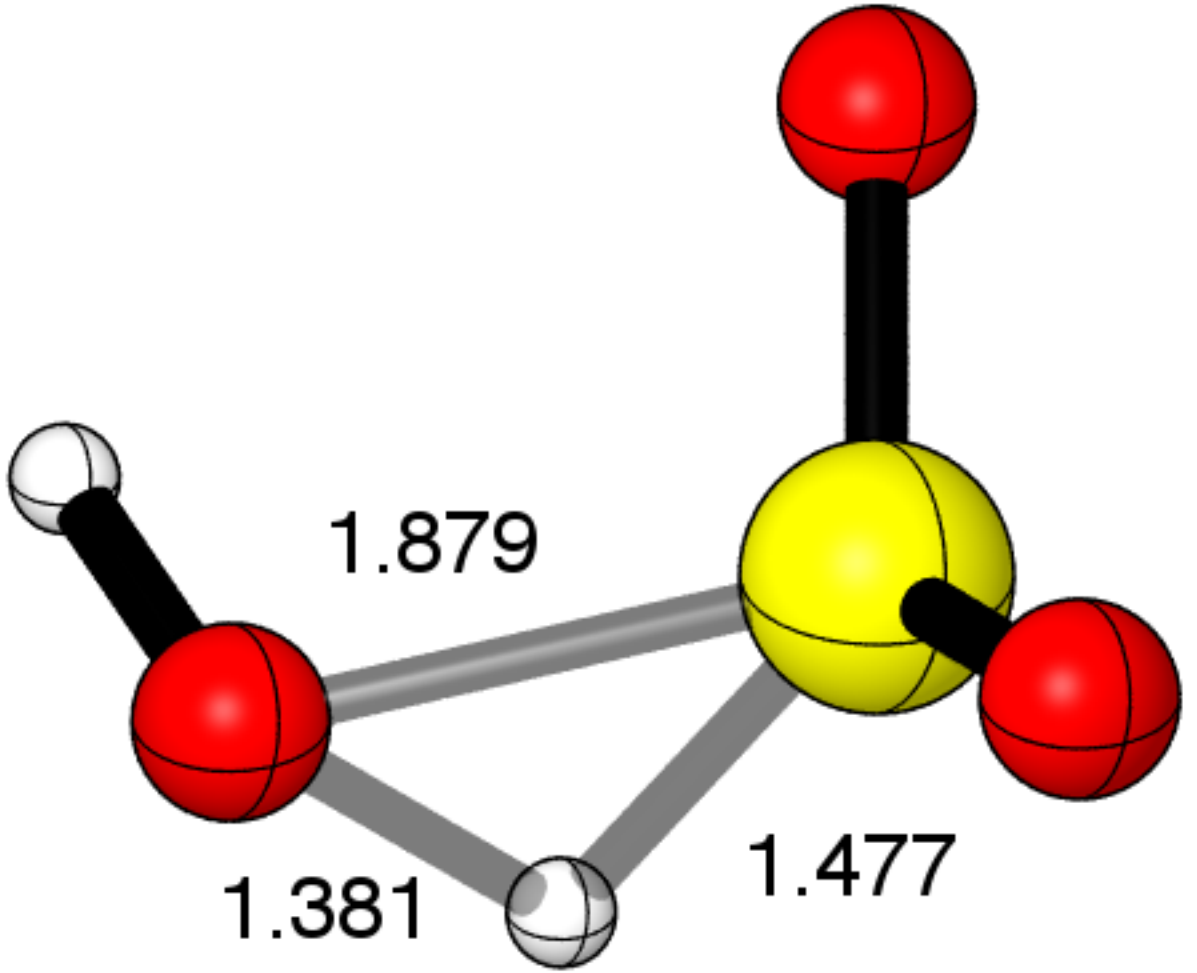
1.879
1.381
1.477

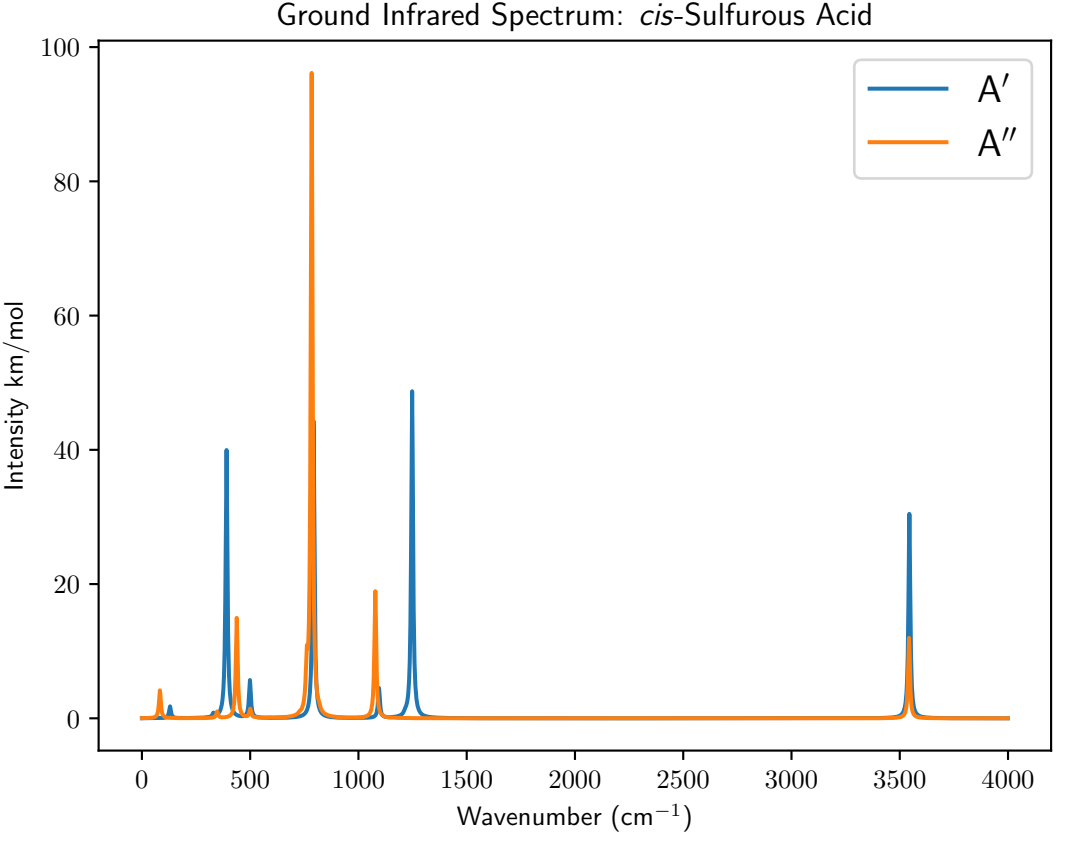
Ground Infrared Spectrum: *cis*-Sulfurous Acid
Intensity km/mol
Wavenumber (cm^{-1})
A′
A″
0
20
40
60
80
100
0
500
1000
1500
2000
2500
3000
3500
4000

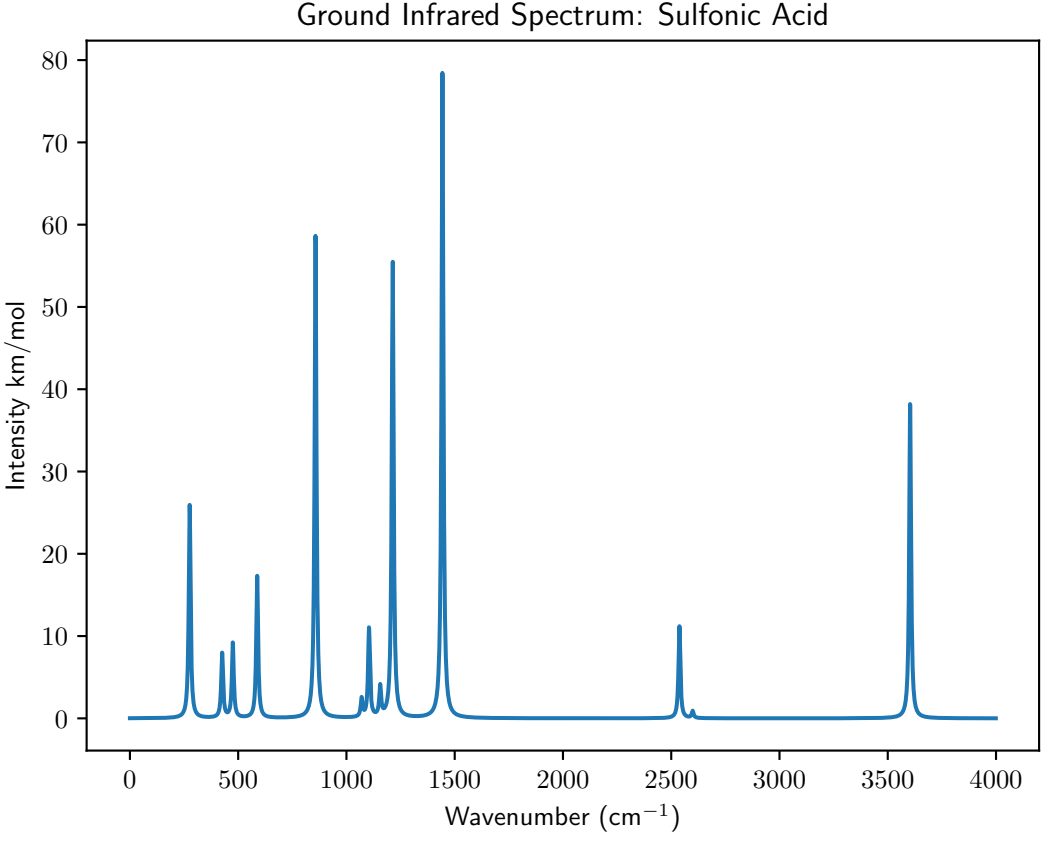
Ground Infrared Spectrum: Sulfonic Acid
Intensity km/mol
Wavenumber (cm^{-1})
0
10
20
30
40
50
60
70
80
0
500
1000
1500
2000
2500
3000
3500
4000

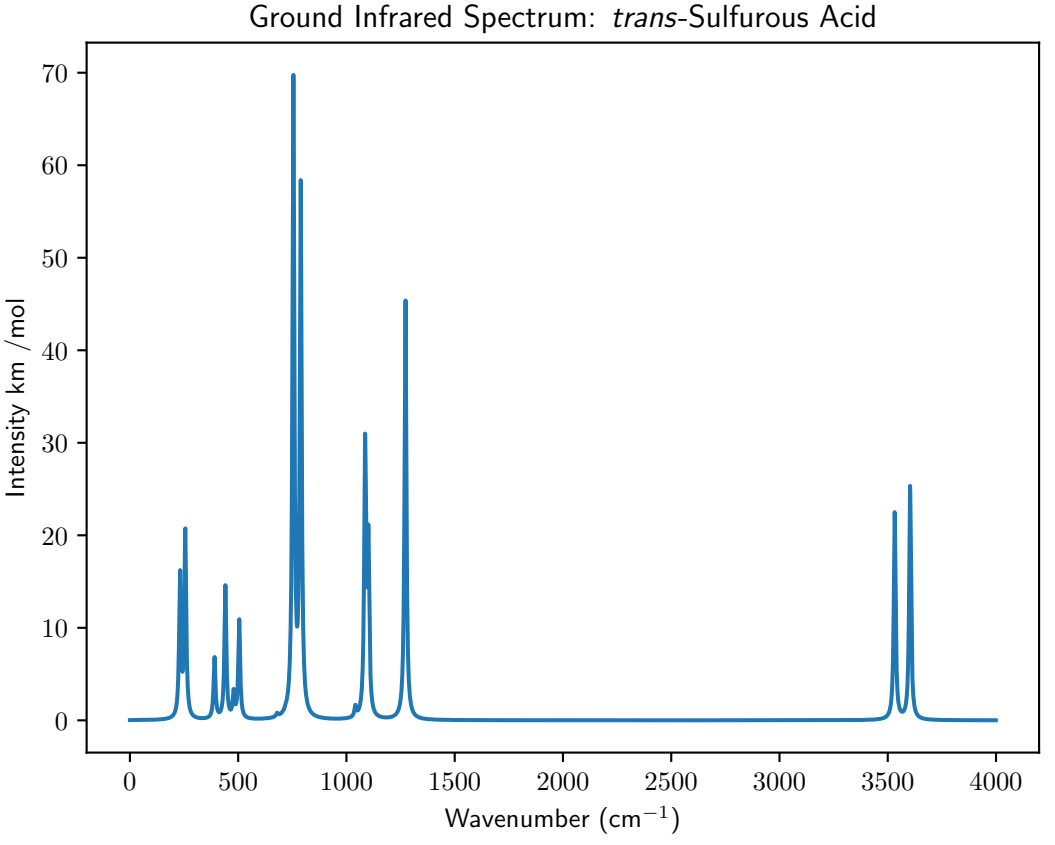
Ground Infrared Spectrum: *trans*-Sulfurous Acid
Intensity km /mol
0
10
20
30
40
50
60
70
0
500
1000
1500
2000
2500
3000
3500
4000
Wavenumber (cm^{-1})

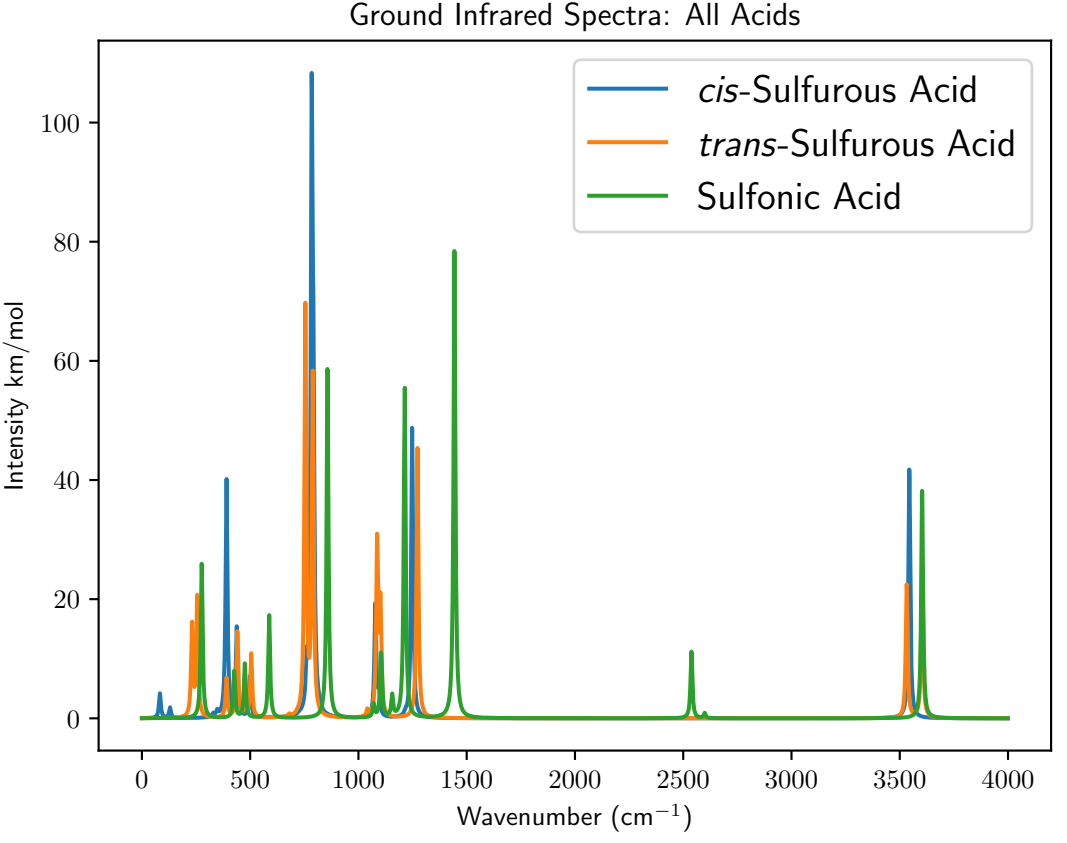
Ground Infrared Spectra: All Acids
cis-Sulfurous Acid
trans-Sulfurous Acid
Sulfonic Acid
Intensity km/mol
0
20
40
60
80
100
0
500
1000
1500
2000
2500
3000
3500
4000
Wavenumber (cm^{-1})